CLASSICAL TWO-DIMENSIONAL METHODS

by

D.S.Whitehead
Whittle Laboratory
Engineering Department
Cambridge University
Adingley Road
Cambridge CB3 0EL
UK

INTRODUCTION

This chapter presents some solutions of the basic equations derived in the previous chapter using methods which have become rather widely used and accepted. The flow is assumed to be two-dimensional, reversible, and isentropic. The methods rely on being able to build up the required flow from simple analytical solutions, and this can be done if either the fluid is incompressible or if the flow contains only small perturbations of a uniform flow. In the latter case the blades are assumed to be flat plates operating at zero incidence, so that the effects of camber and thickness cannot be treated.

The notation used is essentially the same as was used in the chapter "Linearized Unsteady Aerodynamic Theory" by J. Verdon. But the technique of making all variables dimensionless, by scaling with respect to the blade chord (c) and the far upstream velocity (V_∞), will not be used in this chapter because it is felt that in this context there is a gain of physical understanding by working with the dimensional variables. ω is therefore the angular frequency of vibration in radians per second, and a non-dimensional frequency parameter λ will be used, given by $\lambda = \omega c/V_\infty$. In the linearized theory the symbol U will be used as an alternative to V_∞ .

In this chapter no attempt is made to show how the theory has been built up by many authors over several decades. Here, only references to primary sources will be quoted. During the earlier part of the chapter many of these references are to the work of the author of this chapter and his students, and this calls for some apology. But it was felt that only in this way could this author give a reasonably connected account of the theory. There are many other equally valid ways of presenting the material, and the literature is substantial.

UNSTEADY THIN AEROFOIL THEORY, BOUND AND FREE VORTICITY

Consider a cascade of flat plates operating at zero incidence (Figure 1) so that the unsteady effects are small perturbations of a uniform flow. There is a jump in v_x across each blade, and the blades are therefore equivalent to vortex sheets. If γ_t is the total strength of the vortex sheet

$$\gamma_t = v_{x-} - v_{x+} \qquad (1)$$

where the - and + suffices refer to lower and upper surfaces of the blade.

The total circulation round the blade is $\int_0^c \gamma_t \, dx$, and since this

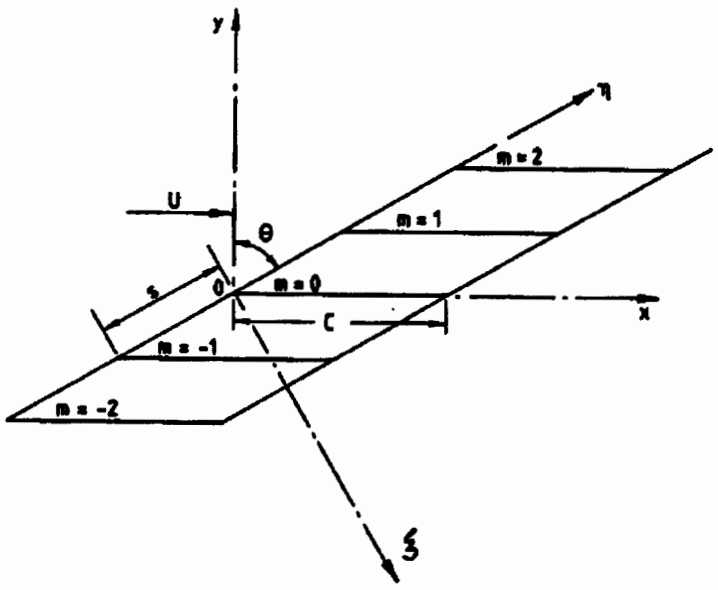

Fig. 1. Notation.

varies sinusoidally with time there will be a vortex sheet shed from the trailing edge which is convected downstream at the mainstream velocity, U .

The whole flow may be considered as being due to the vorticity which replaces the blades and their wakes. The essence of the thin aerofoil theory is to find what vorticity distribution will give the correct upwash velocity so as to satisfy the boundary conditions at the aerofoil surface and in the wake.

Although it is perfectly legitimate to regard the total strength of the vortex sheet γ_t as the primary variable, there is another way which is in practice more convenient. Consider an element of bound vorticity $\gamma(x)\,\delta x\, e^{i\omega t}$ at a point (x,o) on the reference aerofoil. Since the strength varies sinusoidally with time, there will be a sheet of free vorticity $\varepsilon\, e^{i\omega t}$ shed from the element and extending far downstream. During a small time interval δt the strength of the element of bound vorticity changes by an amount

$$\gamma(x)\,\delta x\, e^{i\omega t}\, i\omega\, \delta t .$$

This is equal in magnitude and opposite in sign to the free vorticity appearing in the time δt, during which the shed sheet moves back a distance $U\,\delta t$. Hence just behind the element of bound vorticity, the strength of the sheet of free vorticity is

$$-\frac{\gamma(x)\,\delta x\, e^{i\omega t}\, i\omega\, \delta t}{U \delta t} .$$

Since the whole sheet of free vorticity moves back at the speed, U , the strength at $(x_1\ ,\ 0)$ is

$$\varepsilon(x_1)\, e^{i\omega t} = -\gamma(x)\,\delta x\,\frac{i\omega}{U}\, e^{i\omega\{t+\,(x-x_1)/U\}} . \tag{2}$$

At the point $(x_1\ ,\ 0)$ the sheet of free vorticity gets contributions from all the elements of bound vorticity up to that point. Hence

$$\varepsilon(x_1) = -\frac{i\omega}{U}\int_0^{x_1} \gamma(x)\, e^{i\omega(x-x_1)/U} dx. \tag{3}$$

Multiplying by $e^{i\omega x_1}$, differentiating with respect to x_1 and simplifying gives

$$\frac{d\varepsilon}{dx} + \frac{i\omega}{U}\,(\gamma+\varepsilon) = 0 , \tag{4}$$

or

$$\frac{d\varepsilon}{dx} + \frac{i\omega}{U}\,\gamma_t = 0 ,$$

since the total vorticity γ_t is given by

$$\gamma_t = \gamma + \varepsilon . \tag{5}$$

Writing the linearized x momentum equation for a point just below the blade, and for a point just above the blade and subtracting gives

$$\left(\frac{\partial}{\partial t} + U\frac{\partial}{\partial x}\right)\{(v_{x-} - v_{x+})\, e^{i\omega t}\}$$

$$= -\frac{1}{\rho}\frac{\partial}{\partial x}\,(p_- - p_+)\, e^{i\omega t}$$

$$= \{i\omega(\gamma+\varepsilon) + U\frac{d\gamma}{dx} + U\frac{d\varepsilon}{dx}\}\, e^{i\omega t}$$

$$= U\frac{d\gamma}{dx}\, e^{i\omega t}$$

from Equation (4).

Integrating, and noting that the constant of integration is zero since both γ and $(p_- - p_+)$ are zero off the blade

$$(p_- - p_+) = -\rho U\gamma . \tag{6}$$

It can now be seen why bound vorticity, γ , is a more convenient primary variable than total vorticity γ_t . In the wake γ is zero whereas γ_t is not. Also, in subsonic flow a Kutta condition is applied so that $(P_- - P_+)$ is zero at the trailing edge, and therefore γ is also zero there. In addition, the force and moment on the blade are readily obtained from γ .

$$f_y = \int_o^c (p_- - p_+)\, dx = -\rho U \int_o^c \gamma dx , \tag{7}$$

and

$$m = \int_o^c (p_- - p_+)\, x dx = -\rho U \int_o^c \gamma x dx . \tag{8}$$

Since bound vorticity is equivalent to pressure jump across the blade, theories presented in terms of pressure dipoles, or dipoles of acceleration potential, are formally equivalent to theories presented in terms of bound vorticity.

If an element of bound vorticity $\gamma(x)\,dx$ at the point (x,0) on the reference blade is considered, together with corresponding elements on all other blades, and also the sheets of free vorticity shed from all these elements, then the velocity in the y direction induced at the point (x',0) may be written

$$v_y(x') = \frac{1}{c}\, K\left(\frac{x'-x}{c}\right)\gamma(x)\, dx . \tag{9}$$

Integrating for all elements along the chord

$$v_y(x') = \frac{1}{c}\int_o^c K\left(\frac{x'-x}{c}\right)\gamma(x)\, dx . \tag{10}$$

The evaluation of the kernel function K will be the main concern of the next six sections, but for the present it may be assumed to be known.

The upwash velocity $v_y(x')$ is also known. There are two cases of main interest.

For bending vibration normal to the chord, if the blade displacement is $h_y e^{i\omega t}$ then velocity must match the upwash velocity, so that

$$v_y(x') = i\omega h_y = \dot{h}_y \ . \qquad (11)$$

Bending vibration parallel to the chord has no effect in thin aerofoil theory.

For torsional vibration of the blades about the origin at the leading edge, if the angular displacement is $\alpha\, e^{i\omega t}$ (anticlockwise positive), then the velocity normal to the blade at a distance x' from the axis is

$$(v_y(x') - \alpha U)\, e^{i\omega t} = \frac{d}{dt}\,(x'\alpha\, e^{i\omega t}) \ .$$

Hence

$$v_y(x') = \alpha\,(U + i\omega x') \ . \qquad (12)$$

There are other upwash velocity distributions which are often of interest, due to incoming acoustic waves and incoming vorticity waves. These waves are considered in the sections "Fundamental Acoustic Wave Solutions" and "Vorticity Wave Solutions".

In Equation (10) therefore the v_y function and the K function are known. Equation (10) is therefore an integral equation for the unknown bound vorticity distribution γ . It will be solved numerically by specifying γ at N suitably chosen points along the chord, and then making the upwash velocities match at N other suitably chosen points. More particulars of a solution procedure will be given in the sections "Solution for Subsonic Cascade" and "Solutions for Supersonic Cascade", but first the calculation of the kernel function will be considered.

KERNEL FUNCTION FOR INCOMPRESSIBLE FLOW

If the fluid is assumed to be incompressible, the velocities induced by vortices may be calculated by the Biot-Savart law. The v_y velocity induced at the point $(x', 0)$ by a vortex of strength $\Gamma_m\, e^{i\omega t}$ at the point (x_m, y_m) is

$$v_y = \frac{\Gamma_m}{2\pi}\,\frac{(x' - x_m)}{(x' - x_m)^2 + y_m^2} \ .$$

If the vortex on the reference blade at $(x\ , 0)$ has strength Γ_o , then the strength of the corresponding vortex on the mth blade is given by

$$\Gamma_m = \Gamma_o\, e^{im\sigma} \ ,$$

where σ is the inter-blade phase angle. The position of this vortex is given by

$$x_m = ms\sin\theta + x \ ,$$

$$y_m = ms\cos\theta \ .$$

Summing the effect for all blades gives

$$v_y = \frac{\Gamma_o}{2\pi}\sum_{m=-\infty}^{+\infty} \frac{e^{im\sigma}(x' - x - ms\sin\theta)}{(x'-x-ms\sin\theta)^2+(ms\cos\theta)^2} \ .$$

This may be written

$$v_y = \frac{\Gamma_o}{c}\, V\!\left(\frac{x' - x}{c}\right) \qquad (13)$$

where

$$V(z) = \frac{1}{2\pi}\sum_{m=-\infty}^{+\infty} \frac{e^{im\sigma}\,(z - m\sin\theta\, s/c)}{(z-m\sin\theta s/c)^2+(m\cos\theta s/c)^2}$$

This series can be summed analytically. The result for $0 < \sigma < 2\pi$ is

$$V(z) = \qquad (14)$$

$$\frac{c}{4s}\,\frac{\exp\{-(\pi-\sigma)(\cos\theta + i\sin\theta)\pi c/s + i\theta\}}{\sinh\{\pi\,(\cos\theta + i\sin\theta)\pi c/s\}}$$

$$+$$

$$\frac{c}{4s}\,\frac{\exp\{+(\pi-\sigma)(\cos\theta - i\sin\theta)\pi c/s - i\theta\}}{\sinh\{\pi\,(\cos\theta - i\sin\theta)\pi c/s\}} \ .$$

The case of zero phase angle is special because a row of unsteady vortices produces non-zero induced velocities far upstream and downstream. In order to deal with this case, and have zero induced velocity far upstream of the row of vortices, it is necessary to replace $V(z)$ by $\{V(z)-V(-\infty)\}$.

Equation (13) may be used to evaluate the upwash velocity induced by both the elements of bound velocity γdx, and also the corresponding sheets of free vorticity given by equation (2)

$$v_y(x') = \frac{\gamma dx}{c}\, V\left(\frac{x'-x}{c}\right)$$

$$- \frac{i\omega\gamma dx}{Uc}\int_x^{\infty} e^{i\omega(x-x_1)/U}\, V\!\left(\frac{x'-x_1}{c}\right)dx_1 \ .$$

Comparing this with equation (9) and rearranging gives

$$K(z) = V(z) - i\lambda e^{-i\lambda z}\int_{-\infty}^{z} e^{i\lambda z_1}\, V(z_1)\,dz_1 \qquad (15)$$

where $\lambda = \omega c/U$ is the frequency parameter. This is the required expression for the kernel function in equation (10). The first term gives the effect of the bound vorticity, and the second term gives the effect of the shed sheets of free vorticity.

This is as far as the incompressible solution will be taken, since it is regarded as having been superceded by the methods for subsonic compressible flow. Techniques for solving the integral equation will be discussed in the section "Solution for Subsonic Cascade". A series method for evaluating the infinite integral in equation (15) has been given by Whitehead (1960).

FUNDAMENTAL ACOUSTIC WAVE SOLUTIONS

The equation governing the unsteady velocity potential for small deviations from a uniform mean flow has been derived in the previous chapter by Verdon (equation 133) and is

$$(1 - M2)\frac{\partial^2\phi}{\partial x^2} + \frac{\partial^2\phi}{\partial y^2} - \frac{2i\omega}{A} M \frac{\partial\phi}{\partial x} + \frac{\omega^2}{A^2}\phi = 0,$$

where x and y are measured parallel and perpendicular to the mean flow. Referred to the axial and circumferential axes, coordinates ξ and η, this equation becomes

$$(1-M_\xi^2)\frac{\partial^2\phi}{\partial\xi^2} + (1-M_\eta^2)\frac{\partial^2\phi}{\partial\eta^2} - 2M_\xi M_\eta \frac{\partial^2\phi}{\partial\xi\partial\eta}$$

$$-2\frac{i\omega}{A}\{M_\xi \frac{\partial\phi}{\partial\xi} + M_\eta \frac{\partial\phi}{\partial\eta}\} + \frac{\omega^2}{A^2}\phi = 0 \quad (16)$$

where

$$M_\xi = M \cos\theta,$$

and $$M_\eta = M \sin\theta.$$

The required solution is of the form

$$\phi = \phi\, e^{i(\alpha\xi + \beta\eta)} \quad (17)$$

where α and β are the wave numbers in the axial and circumferential directions.

Substituting this in equation (16) gives

$$\alpha^2 + \beta^2 - (\alpha M_\xi + \beta M_\eta + \omega/A)^2 = 0 . \quad (18)$$

The solution being looked for has a phase angle σ between any blade and its next above neighbour, so that all variables are multiplied by $\exp(i\sigma)$ on going a distance s in the circumferential direction. Hence β is always real and is given by

$$\beta = (\sigma - 2\pi r)/s \quad (19)$$

where r is any integer.

Equation (18) is then a quadratic equation for α, and the solution for α is

$$\alpha = [M_\xi(\beta M_\eta + \omega/A) \pm \{(\beta M_\eta + \omega/A)^2 - (1-M_\xi^2)\beta^2\}^{1/2}]/(1-M_\xi^2) . \quad (20)$$

If $$(\beta M_\eta + \omega/A)^2 - (1 - M_\xi^2)\beta^2 > 0 \quad (21)$$

there are two real roots for α. This corresponds to waves propagating with constant amplitude, and it will be shown that one root corresponds to waves travelling upstream and the other root corresponds to waves travelling downstream (provided $M\xi < 1$).

If $$(\beta M_\eta + \omega/A)^2 - (1 - M_\xi^2)\beta^2 < 0 \quad (22)$$

there are two complex roots for α. One root corresponds to a disturbance which grows exponentially in the axial (positive ξ) direction, and the other root corresponds to a disturbance which decays exponentially in the axial direction.

If $$(\beta M_\eta + \omega/A)^2 - (1 - M_\xi^2)\beta^2 = 0 \quad (23)$$

or

$$\frac{A\beta}{\omega} = \{M_\eta \pm (1-M_\xi^2)^{1/2}\}/(1-M^2) \quad (24)$$

then the waves are just on the verge of propagating. This is known as the "cut-off" or "resonance" condition.

In order to apply the boundary conditions correctly it is necessary to determine the direction in which the propagating acoustic waves carry energy. To do this it is convenient to consider axes $O\xi'\eta'$, which are parallel to the $O\xi\eta$ axes, but which move with the mean velocity of the fluid. Relative to these axes, the wave propagates at a speed A and at an angle ψ as shown in Figure 2. The velocity potential is therefore of the form

$$\phi\, e^{i\omega'(t - \xi'\cos\psi/A - \eta'\sin\psi/A)} \quad (25)$$

where ω' is the intrinsic frequency, the frequency seen by an observer moving with the fluid. Note that the angle ψ gives the inclination of the wavefronts, and is not the direction of energy propagation relative to fixed coordinates.

On switching to fixed axes, $\xi = \xi' + M_\xi At$, $\eta = \eta' + M_\eta At$, so that the potential is

$$\phi\, e^{i\omega t} = \phi\, e^{i(\omega t + \alpha\xi + \beta\eta)}$$

$$= \phi\, e^{i\{(\omega + \alpha M_\xi A + \beta M_\eta A)t + \alpha\xi' + \beta\eta'\}} .$$

Comparing this with equation (25) gives

$$\omega' = \omega + \alpha M_\xi A + \beta M_\eta A , \quad (26)$$

$$\alpha = -\omega'\cos\psi/A , \quad (27)$$

$$\beta = -\omega'\sin\psi/A . \quad (28)$$

If α and β are eliminated from these equations the result is

$$\omega' = \omega/\{1 + M\cos(\theta-\psi)\} . \quad (29)$$

This equation shows that in subsonic flow ω' is always positive, but that in supersonic flow there are some directions of wave propagation (for instance $\psi = \theta+\pi$) for which ω' becomes negative.

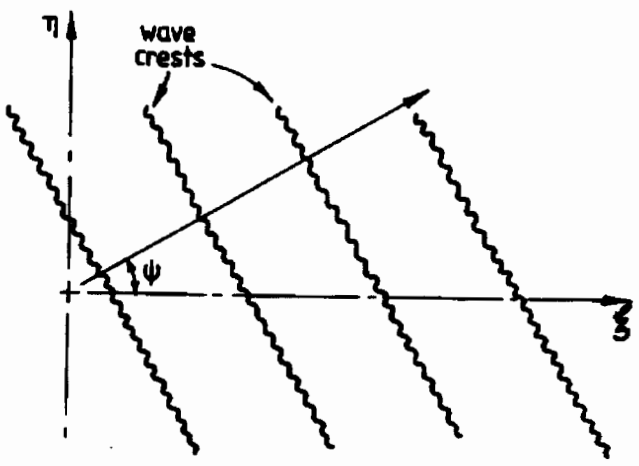

Fig. 2. Wave Propagation.

The group velocity in the axial direction, which is also the rate of axial transfer of wave energy, is then given by the sum of the convection velocity and the axial propagation velocity, and is

$$c_\xi = M_\xi A + A\cos\psi \qquad (30)$$

$$= M_\xi A - A^2\alpha/\omega'$$

$$= \mp \{(\omega + \beta M_\eta A)^2 - (1-M_\xi^2)\beta^2 A^2\}^{1/2}/\omega', \qquad (31)$$

where equations (26) and (20) have been used.

At the resonance or cut-off condition given by equation (23)

$$M_\xi + \cos\psi = 0$$

so that equation (30) shows that $c_\xi = 0$, and the waves carry energy in a purely circumferential direction, so that in a machine the energy propagates round the machine but none is lost by radiation in an axial direction. It will be found that at this point the acoustic waves can reach large amplitudes and the solutions become singular.

In subsonic flow, propagating acoustic waves occur over the range of β given by

$$\frac{M_\eta - (1 - M_\xi^2)^{1/2}}{1 - M^2} < \frac{A\beta}{\omega} < \frac{M_\eta + (1 - M_\xi^2)^{1/2}}{1 - M^2} . \qquad (32)$$

Outside this range decaying waves occur. Within this range, since ω' is always positive, equation (31) shows that the upper sign in equations (20) and (31) corresponds to waves carrying energy upstream, with negative c_x .

If the flow is supersonic ($M>1$), but with subsonic axial velocity ($M_\xi<1$), then propagating acoustic waves occur over the ranges of β given by

$$\frac{A\beta}{\omega} < \frac{-M_\eta - (1 - M_\xi^2)^{1/2}}{M^2 - 1} \qquad (33)$$

and

$$\frac{A\beta}{\omega} > \frac{-M_\eta + (1 - M_\xi^2)^{1/2}}{M^2 - 1} . \qquad (34)$$

Between these two regimes a range of decaying waves occurs. Assuming that $M_\eta>0$, within the range given by equation (33) some analysis shows that ω' is negative for both waves, so that the lower sign in equations (20) and (31) corresponds to waves carrying energy upstream with negative c_x . Within the range given by equation (34), ω' is positive for both waves and the upper sign in equations (20) and (31) corresponds to waves carrying energy upstream.

If the axial velocity is supersonic ($M_\xi > 1$) the waves always propagate, and since c_x is always positive they always carry energy downstream and there is no resonance condition.

For these acoustic waves the velocity perturbations are given by

$$v_\xi = \frac{\partial\phi}{\partial\xi} = i\alpha\phi , \qquad (35)$$

$$v_\eta = \frac{\partial\phi}{\partial\eta} = i\beta\phi . \qquad (36)$$

The pressure perturbation may be obtained from the momentum equation

$$\left(\frac{\partial}{\partial t} + V_\xi \frac{\partial}{\partial\xi} + V_\eta \frac{\partial}{\partial\eta}\right) v_\xi + \frac{1}{\rho}\frac{\partial p}{\partial\xi} = 0 \qquad (37)$$

and is

$$\frac{p}{\rho} = -\frac{\omega' v_\xi}{\alpha} = -\frac{\omega' v_\eta}{\beta} . \qquad (38)$$

Since the fluctuations are isentropic the density perturbation is given by

$$\rho = p/A^2 . \qquad (39)$$

If the effects of incoming acoustic waves are to be calculated, then the sum of the upwash velocities normal to the chord due to the bound and free vorticity, $v_y(x')$ and due to the incoming wave must be zero. Hence

$$v_y(x') - v_{\xi i}\sin\theta + v_{\eta i}\cos\theta = 0$$

where the suffix i refers to the incoming wave. Using equation (38)

$$v_y(x') = \frac{p_i}{\rho U}\,\frac{\beta c\cos\theta - \alpha c\sin\theta}{\lambda + \alpha c\cos\theta + \beta c\sin\theta} .$$

This can be evaluated for each of the pair of the waves corresponding to a given value of β . For unit value of $p_i/\rho U$ at the origin

$$v_y(x') = \frac{\beta c\cos\theta - \alpha c\sin\theta}{\lambda + \alpha c\cos\theta + \beta c\sin\theta} \cdot \exp i(\alpha\cos\theta + \beta\sin\theta)x' \qquad (40)$$

VORTICITY WAVE SOLUTIONS

In addition to the acoustic wave solutions discussed in the last section, the continuity and momentum equations also admit of solutions which include vorticity, but have no pressure or density perturbation. For these solutions the velocity potential does not exist and the disturbances are convected downstream at the mean fluid velocity. These solutions therefore have

$$p = 0, \quad \rho = 0 . \qquad (41)$$

The required solution is of the form

$$v_\xi e^{i\omega t} = \text{const}\; e^{i(\omega t + \alpha\xi + \beta\eta)}$$

Putting these in the momentum equation (37) gives

$$\omega + V_\xi\alpha + V_\eta\beta = 0,$$

so that

$$\alpha = -(\omega + V_\eta\beta)/V_\xi . \qquad (42)$$

Since there is no density perturbation, the continuity equation can be used in its incompressible form

$$\frac{\partial v_\xi}{\partial\xi} + \frac{\partial v_\eta}{\partial\eta} = 0,$$

to give

$$\alpha v_\xi + \beta v_\eta = 0. \qquad (43)$$

Since these vorticity wave solutions have no pressure or density perturbations, they are unaffected by compressibility effects and apply at all Mach numbers.

The force and moment on the blades, due to wakes from some obstructions upstream which are in motion relative to the blades, are often required in order to calculate the forced vibration. A Fourier analysis of the wake profile in the η direction may be carried out, and each term corresponds to a vorticity wave of the type considered in this section. The sum of the upwash velocities normal to the chord due to the bound and free vorticity, $v_y(x')$ and due to the incoming vorticity wave must be zero.

Hence

$$v_y(x') - v_{\xi i} \sin\theta + v_{\eta i} \cos\theta = 0,$$

where the suffix i refers to the incoming wave.

Using equations (42) and (43) this gives for a velocity v_w normal to the chord at the origin

$$\begin{aligned} v_y(x') &= - v_w \exp(-i\omega x'/U) \\ &= - v_w \exp(-i\lambda x'/c), \end{aligned} \qquad (44)$$

showing how the waves are convected along the chord at the mainstream velocity.

KERNEL FUNCTION FOR SUBSONIC CASCADE

The incompressible kernel function which was derived in the section "Kernel Function for Incompressible Flow" of this chapter was based on the replacement of the aerofoils of the cascade by a number of bound vortices. In that case the effect of a row of bound vortices, with the spacing and stagger corresponding to the cascade in question, could be obtained by summing the series analytically. The corresponding solution in subsonic compressible flow for a single bound vortex involves Hankel functions, and when the series for a row of such vortices is written down it appears that it cannot be summed analytically, and if numerical evaluation of the series is attempted the series is found to converge very badly. The approach that will be used is therefore to build up the solution for the row of vortices from the acoustic and vorticity wave solutions given in the sections "Fundamental Acoustic Wave Solutions" and "Vorticity Wave Solutions". The presentation largely follows the paper by Smith (1972).

Consider therefore a row of vortices spread along the η axis with spacing s and phase angle σ. This may be considered as a distribution of bound vorticity along the η axis given by

$$\gamma = \sum_{m=-\infty}^{+\infty} \Gamma_0 e^{im\sigma} \delta(\eta - ms). \qquad (45)$$

This series of delta functions may be transformed to a Fourier series as follows

$$\gamma = \Gamma_0 e^{i\eta\sigma/s} \sum_{m=-\infty}^{+\infty} e^{-i(\eta-ms)\sigma/s} \delta(\eta-ms)$$

$$= \Gamma_0 e^{i\eta\sigma/s} \sum_{m=-\infty}^{+\infty} \delta(\eta-ms)$$

since the delta function is only non-zero when $\eta - ms = 0$. Hence

$$\gamma = \Gamma_0 e^{i\eta\sigma/s} (1/s) \sum_{r=-\infty}^{+\infty} e^{-i2\pi r\eta/s}$$

by example 38 of Lighthill (1958). Hence

$$\gamma = \frac{\Gamma_0}{s} \sum_{r=-\infty}^{+\infty} e^{i(\sigma-2\pi r)\eta/s}. \qquad (46)$$

Each term of this series is sinusoidal in the η direction, and therefore the solutions of the sections "Fundamental Acoustic Wave Solutions" and "Vorticity Wave Solutions" may be matched to it. Upstream of the row of vortices only the upstream going acoustic wave, or alternatively the wave which decays exponentially upstream, can exist, and this will be distinguished by the suffix 1. Downstream of the row, only the downstream going acoustic wave, or alternatively the wave which decays exponentially downstream, can exist, and this will be distinguished by the suffix 2. In addition, downstream of the row there will be a vorticity wave, and this will be distinguished by the suffix 3.

Considering then just one term of the series in equation (46) three conditions are necessary to find these waves. Firstly, continuity may be applied across the vortex sheet at $\xi = 0$, so that

$$\begin{aligned} &(V_\xi + \tilde{v}_{\xi 1})(\bar{\rho} + \tilde{\rho}_1) = \\ &(V_\xi + \tilde{v}_{\xi 2} + \tilde{v}_{\xi 3})(\bar{\rho} + \tilde{\rho}_2), \end{aligned}$$

or, to first order in the perturbations,

$$\bar{\rho} v_{\xi 1} + V_\xi \tilde{\rho}_1 = \bar{\rho} v_{\xi 2} + \bar{\rho}\, v_{\xi 3} + V_\xi\, \tilde{\rho}_2 . \qquad (47)$$

Secondly, the velocity jump across the row in the η direction must be equal to the strength of the sheet of bound vorticity, so that, for a sheet of unit amplitude

$$v_{\eta_2} + v_{\eta_3} - v_{\eta_1} = 1. \qquad (48)$$

Thirdly, the strength of the vorticity wave may be related to the strength of the sheet of bound vorticity from which it is shed. In a time interval δt, the circulation shed from an element of bound vorticity $\gamma\, d\eta$ is

$$- \frac{d}{dt}(\gamma\, d\eta)\, \delta t = \zeta_3\, d\eta\, (V_\xi\, \delta t)$$

where ζ_3 is the vorticity just downstream, and this is spread over an area $d\eta$ in the η direction and $(V_\xi\, \delta t)$ in the ξ direction. Hence

$$\zeta_3 = - i\omega\gamma / V_\xi .$$

But

$$\begin{aligned} \zeta &= \frac{\partial v_\eta}{\partial \xi} - \frac{\partial v_\xi}{\partial \eta} \\ &= i\alpha v_\eta - i\beta v_\xi . \end{aligned}$$

Hence, for a sheet of unit amplitude,

$$\alpha_3 \, v_{\eta 3} - \beta \, v_{\xi 3} = - \omega / V_\xi \, . \qquad (49)$$

Equations (47), (48) and (49) may now be solved to give the velocity perturbations for the acoustic waves and the vorticity wave just upstream and downstream of the $\xi = 0$ axis. Equations (38) and (39) are used to relate the acoustic perturbations, and equation (43) is used for the vorticity wave. The wave numbers in the axial direction are given by equations (20) and (42). The results are

$$v_{\eta_3} = (\lambda^2 + \lambda\beta c \sin\theta)/A' \, , \qquad (50)$$

$$v_{\eta_1} = (\beta c/2A') \{-(\beta c + \lambda \sin\theta) + \lambda\beta c \cos\theta(-E)^{-1/2}\} \, . \qquad (51)$$

$$v_{\eta_2} = (\beta c/2A') \{+(\beta c + \lambda \sin\theta) + \lambda\beta c \cos\theta(-E)^{-1/2}\} \, . \qquad (52)$$

where

$$A' = \lambda^2 + \beta^2 c^2 + 2\lambda\beta c \sin\theta \qquad (53)$$

and

$$E = \beta^2 c^2 - M^2 A' \, . \qquad (54)$$

Equations (51) and (52) are written for propagating waves ($E < 0$) . For decaying waves ($E > 0$) $(-E)^{-1/2}$ is replaced by $i(E)^{-1/2}$. The corresponding v_ξ velocity perturbations are obtained from equations (38) and (43).

The velocities induced in the y direction normal to the blade chord at the point $\xi = x'\cos\theta$, $\eta = x'\sin\theta$, by the row of bound vortices at $\xi = 0$ may therefore be written, for $x' < 0$ (upstream of the row)

$$v_y = \frac{\Gamma_0}{s} \sum_{r=-\infty}^{+\infty} (v_{\eta_1} \cos\theta - v_{\xi_1} \sin\theta) \, e^{i(\alpha_1 \cos\theta + \beta \sin\theta)x'} \, .$$

Comparing this with equation (10) shows that the kernel function is given by

$$K(z) = \frac{c}{s} \sum_{r=-\infty}^{+\infty} (v_{\eta_1} \cos\theta - v_{\xi_1} \sin\theta) \, e^{i(\alpha_1 \cos\theta + \beta \sin\theta)cz} \qquad (55)$$

for $z < 0$.

The corresponding expression for downstream of the row of vortices includes the effect of the vorticity waves, so that

$$K(z) = \frac{c}{s} \sum_{r=-\infty}^{+\infty} (v_{\eta_2} \cos\theta - v_{\xi_2} \sin\theta) \, e^{i(\alpha_2 \cos\theta + \beta \sin\theta)cz} + \frac{c}{s} \sum_{r=-\infty}^{+\infty} (v_{\eta_3} \cos\theta - v_{\xi_3} \sin\theta) \, e^{i(\alpha_3 \cos\theta + \beta \sin\theta)cz} \qquad (56)$$

for $z > 0$.

It has been shown that propagating waves only occur for a limited range of β , and that outside this range the waves decay. Hence large values of r (positive or negative) give large value of $|\beta|$, and the effect decays very rapidly on going away from the row of vortices. The two series for the acoustic waves therefore show good convergence, with terms decaying exponentially as $|r|$ increases. However, the convergence is less good when z is small, but still very satisfactory.

The second series for the vorticity waves in equation (56) does not show satisfactory convergence. However, Smith (1972) shows that this series may be summed analytically. The result for the kernel function may then be written

$$K(z) = \frac{c}{s} \sum_{r=-\infty}^{+\infty} (v_{\eta_2} \cos\theta - v_{\xi_2} \sin\theta) \, e^{i(\alpha_2 \cos\theta + \beta \sin\theta)cz} + \frac{\lambda}{2} \frac{\sinh(\lambda \cos\theta \, s/c) \exp(-i\lambda z)}{\cosh(\lambda \cos\theta \, s/c) - \cos(\sigma + \lambda \sin\theta \, s/c)} \qquad (57)$$

for $z > 0$.

SOLUTION FOR SUBSONIC CASCADE

In order to complete the analysis it is necessary to solve numerically the integral equation (10). In subsonic flow this has to be done subject to the Kutta condition at the trailing edge, which says that the pressure difference across the blade must tend to zero as the trailing edge is approached.

The bound vorticity, γ , will be specified at N points and perhaps the obvious way to do this would be to take these points equally spaced along the chord. But it has been found that a great increase in accuracy, using a modest value of N , can be obtained using the transformation (as in the classical thin-aerofoil theory of isolated aerofoils).

$$x = \tfrac{1}{2} c \, (1 - \cos\psi). \qquad (58)$$

Then γ is specified at points given by

$$\psi = \pi l/N \qquad (59)$$

where l is an integer $0 < l < (N-1)$. It will be noted that this does not include the point at the trailing edge ($x = c$, $\psi = \pi$, $l = N$) , since, by the Kutta condition, γ is zero there.

The upwash velocities will then be matched at points given by

$$x' = \tfrac{1}{2} c \, (1 - \cos\epsilon) \qquad (60)$$

where

$$\epsilon = \pi(2m + 1)/(2N) \qquad (61)$$

and m is an integer $0 < m < (N - 1)$.

These points have values of ϵ halfway between the values of ψ at which the bound vorticity is specified.

Making these substitutions in equation (10) gives

$$v_y(\varepsilon) = \frac{1}{2}\int_0^{\pi} K\left(\frac{1}{2}(\cos\psi - \cos\varepsilon)\right)\gamma(\nu)\sin\psi\, d\psi. \quad (62)$$

These substitutions remove a difficulty at the leading edge ($x = 0$, $\psi = 0$), since in the solution γ becomes infinite at that point. But by regarding $\gamma\sin\psi$ as the fundamsntal variable this product remains finite at the leading edge and causes no numerical difficulty. These substitutions also remove the singularity at the leading edge in integrals for the blade force and moment in equations (7) and (8), which were

$$f_y = -\frac{1}{2}\bar{\rho}\, U\, c\int_0^{\pi}\gamma(\nu)\sin\psi\, d\psi \quad (63)$$

$$m = -\frac{1}{4}\bar{\rho}\, U\, c^2\int_0^{\pi}\gamma(\psi)\sin\psi\,(1-\cos\psi)d\psi. \quad (64)$$

With the reservation to be made shortly the integrals in equations (62) (63) and (64) may be evaluated by the trapezoidal rule. Expressing the results in matrix form, equation (62) becomes

$$\underline{U} = \underline{K}\,\underline{\Gamma} \quad (65)$$

where $\underline{U}$ is an upwash matrix having N rows and 2 columns. The first column gives the upwash velocity due to bending for unit (h_y/U) and the second column gives the upwash velocity due to torsion for unit α. According to equations (11) and (12)

$$\underline{U} = [1,\ (1 + i\lambda x'/c)]\ . \quad (66)$$

Further columns may be added for incoming acoustic waves from upstream or downstream, and for incoming vorticity waves, if these results are required.

$\underline{K}$ is a kernel matrix (N x N) where elements are given by $K(1/2(\cos\psi - \cos\varepsilon))$.

$\underline{\Gamma}$ is a bound vorticity matrix having N rows and two (or more) columns whose elements are given by

$$\underline{\Gamma} = [(\pi/2N)(\gamma/U)\sin\psi] \quad (67)$$

except for the first row which has half weight.

Equations (63) and (64) may similarly be written in matrix form

$$\underline{C} = \underline{X}\,\underline{\Gamma} \quad (68)$$

where

$$\underline{C} = \begin{bmatrix} (f_y/\bar{\rho}Uch_y & (f_y/\bar{\rho}U^2c\alpha) \\ (m/\bar{\rho}Uc^2h_y & (m/\bar{\rho}U^2c^2\alpha) \end{bmatrix}, \quad (69)$$

and

$$\underline{X} = [-1 \qquad -\tfrac{1}{2}(1-\cos\psi)]. \quad (70)$$

Further columns may be added to $\underline{C}$ for additional input waves, and further rows may be added to $\underline{X}$ and $\underline{C}$ to give additional outputs, such as the strength of the vortex sheets shed from the blades, and outgoing acoustic waves.

Equation (65) may be formally solved for $\underline{\Gamma}$, and substituted into equation (68) to give the final result

$$\underline{C} = \underline{X}\,\underline{K}^{-1}\,\underline{U}. \quad (71)$$

One important complication concerns the singularities of the kernel function $K(z)$ at $z = 0$. Smith (1972) shows that these are of the form

$$\frac{b^2}{2\pi z} - \frac{\lambda}{2\pi b}\left(1 + a_1\lambda z - ia_2\lambda^2z^2 - a_3\lambda^3z^3 + \ldots.\right)\mathrm{Log}|z|$$

where

$$a_1 = 1 - M^2/2b^2$$

$$a_2 = 1 - 1/2b^2 + M^2/4b^4$$

$$a_3 = \tfrac{1}{2}(1 - 1/b^2 + M^2/6b^2 + 1/3b^4 - 3M^4/8b^6 + M^6/6b^6)$$

and

$$b^2 = 1 - M^2\ .$$

Whitehead (1960) has shown that integration of the $1/z$ singularity is accurately handled by the trapezoidal rule, but that a correction is required for the $\mathrm{Log}|z|$ singularity if accurate results are to be obtained with modest values of N. Reference may be made to the original papers for the details of this correction.

A Fortran computer program for the implementation of this subsonic solution is given in Appendix A.

SOLUTIONS FOR SUPERSONIC CASCADE

When the mainstream is supersonic, the same general approach may be used as in the subsonic case, but there are a number of features which make the solution very different. There are also fundamental differences between the case when the axial velocity is subsonic and when the axial velocity is supersonic. If the axial velocity is supersonic the effects of an element of bound vorticity or pressure dipole introduced at any point are entirely downstream of that point. There is no effect upstream of the leading edge plane, and the flow can in principle be calculated by the method of characteristics. But if the axial velocity is subsonic, then a pressure dipole introduced on one blade implies other pressure dipoles on the blades below it, and the effects of these dipoles go upstream of the original dipole. The flow is therefore one in which upstream effects are possible and it has some of the features of a subsonic flow. There is an effect upstream of the leading edge plane, and the flow cannot be calculated in a straightforward way by the method of characteristics since there is no region of known flow from which to start. The supersonic axial velocity case very seldom occurs in real turbomachines, and is therefore of mainly academic interest. Attention will therefore be concentrated here on the subsonic axial velocity case.

Another difference between the subsonic and supersonic cases is that in the supersonic case no Kutta condition is applicable. The pressures across the wake are equalized by waves emanating from the trailing edge, and just upstream of the trailing edge there is a finite pressure jump across the blade. Conversely, at the leading edge the pressure jump is finite, and not infinite as it is in subsonic flow.

Waves of finite strength originate from the leading and trailing edges of the blades. These waves may be reflected from the surfaces of adjacent blades, and some of the patterns which result are illustrated in Figure 3. Diagrams (a) to (d) apply for the subsonic axial velocity case, and diagrams (e) to (h) apply for the supersonic axial velocity case. In Figure 3a all the waves from one blade go ahead of the blade above it and behind the blade below it, so there are no reflections. In steady flow there is no interference between blades, but in unsteady flow each blade can influence the flow over the blades above it. Figure 3b shows a trailing edge wave reflected once. Figure 3c shows a trailing edge wave reflected once and a leading edge wave reflected twice: this is the usual design case for a fan tip section. Figure 3d shows four reflections of a leading edge wave, and by extending the blade chord the number of reflections can be increased indefinitely, but these cases are not of much practical importance.

Figures 3(e) to (h) show the supersonic axial velocity cases, and the trailing edge waves always go downstream of all other blades. In Figure 3(e) the leading edge waves also go downstream and there is no interference between blades which all behave like isolated aerofoils. Figure 3(f) shows one reflection of a leading edge wave, and Figure 3(g) shows one reflection of both of the leading edge waves, and Figure 3(h) shows two reflections of both of the leading edge waves. Again there are theoretical possibilities with large numbers of reflections.

In order to illuminate the most important features of the flow we shall start with a simple quasi-steady analysis. Torsional vibration is considered, and it is supposed that the blades have moved to a position consistent with a prescribed phase angle σ between blades and are then frozen in that position.

Standard supersonic thin aerofoil theory will be used, so that the relationship between the pressure change (Δp) across a weak wave and the corresponding deflection ($\Delta\theta$) of the flow is

$$\frac{\Delta p}{\rho U^2} = \pm \frac{\Delta\theta}{B} \qquad (72)$$

where $B^2 = (M^2 - 1)$ and the positive sign applies to an upward going wave and the negative sign to a downward going wave.

Since the blades are flat plates, waves originate only from the leading and trailing edges of the blades. They may then be reflected from the adjacent blades, as already discussed and illustrated in Figure 3.

A wave starting downwards from the leading edge of one blade hits the next blade below at a point distant d_1 downstream from its leading edge, where

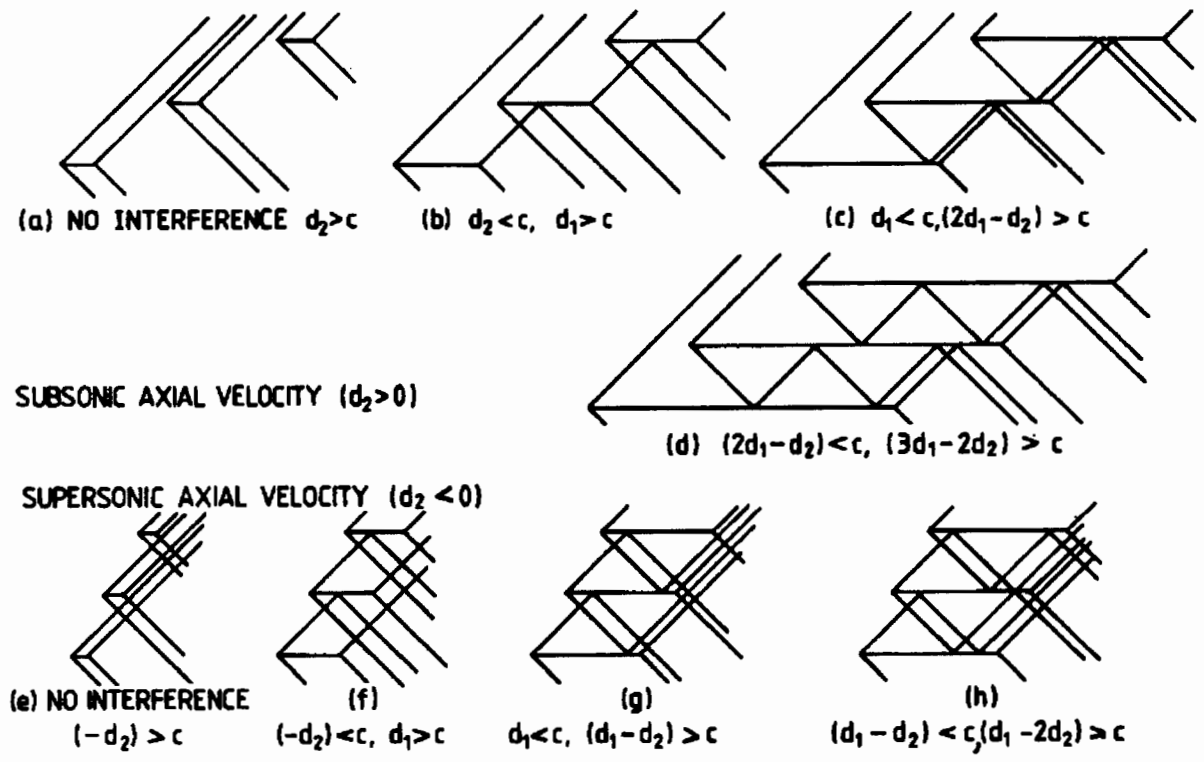

Fig. 3. Wave Reflection Patterns.

$$d_1 = s(\sin\theta + B\cos\theta) \ . \qquad (73)$$

Similarly a wave starting upwards from the leading edge of one blade reaches the y position of the next blade above at a point distant d_2 upstream of its leading edge, where

$$d_2 = s(\sin\theta - B\cos\theta) \ . \qquad (74)$$

If the axial velocity is supersonic, d_2 is negative.

We consider first cases with a subsonic axial velocity, such as (b) and (c) in Figure 3, but exclude case (a). Case (c) is illustrated on a larger scale in Figure 4. Let L be the strength, measured by the increase in pressure, of the wave going upwards from the leading edge of blade $m = 0$, and let T be the strength of the wave going upwards from the trailing edge. Then waves of strength -L and -T go downwards from the leading and trailing edges respectively.

Just ahead of the blade $m = 0$, the flow angle must match the angle of blade $m = -1$, just below, and is $\alpha \exp(-i\sigma)$. Just behind the wave of strength L going upward from the leading edge blade $m = 0$, the flow angle must match the angle of blade $m = 0$, and is α . Hence from equation (72),

$$\frac{L}{\rho U^2} = + \frac{\alpha - \alpha \exp(-i\sigma)}{B} = \frac{\alpha}{B}(1 - \exp(-i\sigma)). \qquad (75)$$

This determines the strength of the leading edge wave. It is zero if $\sigma = 0$. It does not depend on the number of internal wave reflections.

Bearing in mind that a wave is reflected from a solid surface as a wave of the same strength, the pressure in each area between waves may now be written down, and these are shown in square boxes on Figure 4 relative to the pressure ahead of the blade $m = 0$. It will be noted that the pressure jump across each blade has three discontinuities along the chord.

The strength of the trailing edge wave, T , may now be determined from the condition that the pressures on each side of the wake behind the blade must be equal. This gives

$$L - 2L\,e^{i\sigma} + T = -3L + 2Te^{-i\sigma} - T \ .$$

Hence

$$T = -\frac{2 - e^{i\sigma}}{1 - e^{-i\sigma}} L \ . \qquad (76)$$

If $\sigma = 0$, then $L = 0$ and T becomes indeterminate. The case $\sigma = 0$ must therefore be excluded from the present analysis. It will be handled by actuator disc methods in section "Actuator Disk Theory."

Apart from this case equations (75) and (76) give

$$\frac{T}{\rho U^2} = -\frac{\alpha}{B}(2 - e^{i\sigma}) \ . \qquad (77)$$

The force on the blade $m = 0$ may now be determined, and is

$$f_y = -L(d_1 - d_2) - 3L(c - d_1) + (-3L + 2Te^{-i\sigma})d_2 - Ld_1 - (L - 2Le^{i\sigma})(c - d_1) \ .$$

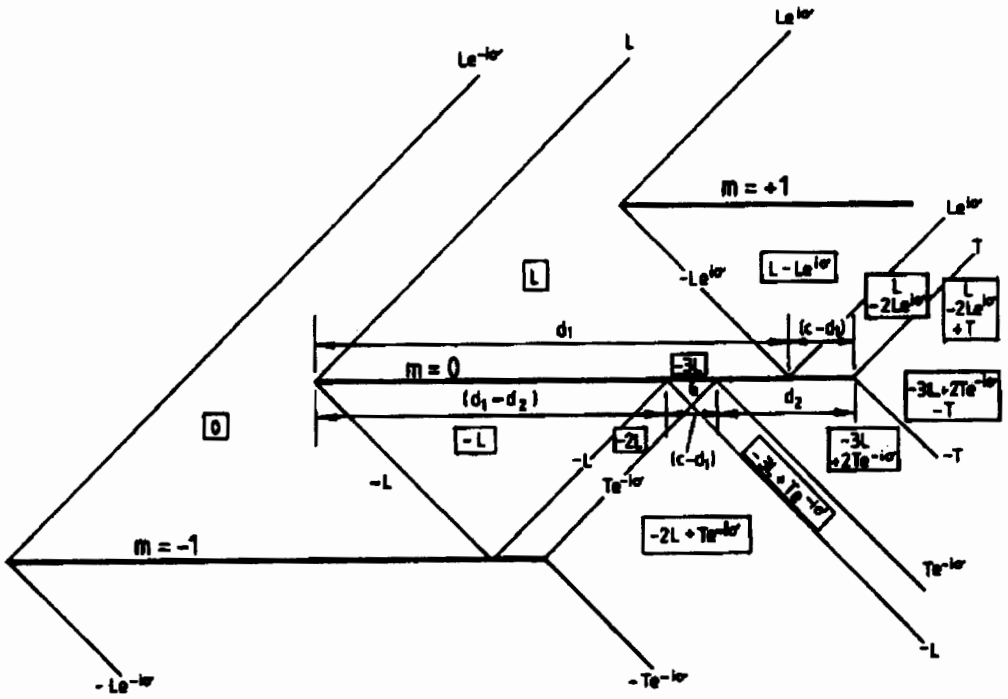

Fig. 4. Detail of Pressure Field for Case (c).

This gives for case (c)

$$fy/\bar{\rho}U^2c\alpha = -\frac{2}{B}\{1 - e^{-i\sigma(1-d_2/c)} + 2(1-\cos\sigma)(1-d_1/c)\} \quad (78)$$

and the moment about the leading edge is similarly given by

$$m/\bar{\rho}U^2c^2\alpha = -\frac{1}{B}\{1 - e^{-i\sigma(1-d_2/c)^2} + 2(1-\cos\sigma)(1 - d_1/c)(1 + d_1/c-d_2/c) - 2i\sin\sigma\,(1 - d_1/c)(d_2/c)\} . \quad (79)$$

Results for other cases of wave reflections may be obtained in a similar way. For cases (a) and (e) in Figure 3, when there is no inter-blade effect,

$$fy/\bar{\rho}U^2c\alpha = -\frac{2}{B} \quad (80)$$

and

$$m/\bar{\rho}U^2c^2\alpha = -\frac{1}{B} . \quad (81)$$

For subsonic axial velocity and for the general case when a wave starting downwards is reflected R times from the blade below and R times by the original blade, R is an integer given by

$$(R-1) < \frac{c-d_1}{d_1-d_2} < R . \quad (82)$$

R = 0 corresponds to case (b) (Figure 3), R = 1 corresponds to case (c) and R = 2 to case (d).

The strength of the leading edge waves is given by equation (75), and the strength of the trailing edge waves is

$$T/\bar{\rho}U^2 = -\frac{\alpha}{B}(1 + R(1 + e^{i\sigma})) . \quad (83)$$

The blade force is given by

$$fy/\bar{\rho}U^2c\alpha = -\frac{2}{B}[1 - e^{-i\sigma(1-d_2/c)} + (1-\cos\sigma)R\{2(1-d_2/c) - (R+1)(d_1-d_2)/c\}], \quad (84)$$

and the moment about the leading edge is

$$m/\bar{\rho}U^2c^2\alpha = -\frac{1}{B}[1 - e^{-i\sigma(1-d_2/c)^2} + (1-\cos\sigma)R\{2(1-d_2/c)-d_2(d_1-d_2)(R+1)/c^2 - (d_1-d_2)^2(R+1)(2R+1)/(3c^2)\} - (i\sin\sigma)R\{2(1-d_2/c)(d_2/c) - d_2(d_1-d_2)(R+1)/c^2\}] \quad (85)$$

These results have been written for torsion, but they also apply to bending with $U\alpha$ replaced by h_y, since equations (11) and (12) show that when $\omega = 0$ the upwash velocities are then identical. They also apply to the effect of wakes from upstream obstructions, since equation (44) shows that when $\omega = 0$ the upwash velocity is also uniform.

The results are essentially those derived by Kurosaka (1973) and by Strada, Chadwick, and Platzer (1979) and by Nagashima and Whitehead (1977), using different methods. These papers also give formulae valid when the frequency is small, but not zero, and correct to first order in ω. However, it appears that some of the terms in these formulae are not entirely in agreement between the three papers.

Nagashima and Whitehead (1977) also give formulae for force and moment in the case of $\omega = 0$ for supersonic axial velocity.

Turning to the full unsteady case with a frequency which is not small, all the available theories are complicated. Therefore, only a brief qualitative introduction to these methods will be given here. The most straightforward approach is to use a semi-infinite cascade, assuming that there is no perturbation upstream of a first blade. The flow may then be solved by the method of characteristics, (Brix and Platzer, 1974), or by finite difference methods (Verdon, 1973). The number of blades in the cascade must be chosen sufficiently large for the blade force and moment to approach limiting values. This involves large computation times, since the convergence with increasing blade number is slow. Also it appears that the results for the unsteady pressures on the surface of the blades converge much more slowly than the results for the blade loadings (Strada, Chadwick, and Platzer, 1979).

Calculations for an infinite cascade at realistic frequencies must include two physical effects. The first of these is the reflections of the leading and trailing edge waves from the adjacent surfaces, as already discussed in the case of steady flow. The second is the acoustic resonance effect, as discussed in the section "Fundamental Acoustic Wave Solutions." For a certain range of phase angles, all possible acoustic waves will propagate, and this regime is sometimes called the "subresonant" regime. The range of the phase angles where one or more of the possible acoustic waves are of exponentially decaying type is then called the "super-resonant" regime. This regime normally occurs for negative interblade phase angles, when the wave of elastic vibration of a fan rotor travels in the opposite direction to the direction of rotation, and is therefore classified as a "backward-travelling" wave.

A calculation in a single blade passage, with the correct blade-to-blade periodicity condition, has been given by Verdon and McCune (1975). The solution is formulated in terms of the velocity potential, and the kernel function is evaluated as a series of Bessel functions. The internal reflections are treated explicitly, and iteration is necessary to deal with the influence of the wake from one blade on the rear part of the lower surface of the blade above. This convergence fails in the "super-resonant" region. This limitation has been removed by Verdon (1977) by using a formulation in terms of pressure to find

the unsteady loading on the lower surface behind the point at which the Mach wave from the trailing edge of the next blade below hits the lower surface.

Formulations in terms of pressure, which relate more closely to the subsonic solution given in the previous section, have been given by Nagashima and Whitehead (1977) and by Ni (1979). If an attempt is made to calculate the kernel function by the series given in (55) it is found that the series does not converge. This behaviour is related to the jump changes in pressure across the waves propagated from the sources. The technique used is therefore to subtract out the steady and quasi-steady terms from the series in (55), to leave a series which does converge, and this is done in two different ways in these two papers. It is also necessary to allow for the reflections of the waves within the blade passage explicitly. In supersonic flow there is no point in using the transformations given in (58) and (60), and uniform spacing along the chord seems to be best for the points at which the bound vorticity is specified and for the points at which the upwash velocities are matched.

A quite different approach has been used by Adamczyk and Goldstein (1978). The problem is split into two parts. The first part consists of the inlet region, followed by a cascade of plates having the same spacing and stagger angle as the actual cascade, but with the chord extending to $x = +\infty$. The second part consists of the exit region, preceded by a cascade of flat plates with the chord extended back to $x = -\infty$. These two parts are then solved by two separate applications of the Wiener-Hopf technique. The solutions are then combined to give a solution of the complete problem.

Computer programs based on these last four very different methods have been shown to give identical results. Some specimen results will be presented in the section "Specimen Results for Flat Plate Cascades."

TRANSONIC THEORY

The equation governing small deviations from a uniform flow has been given by Verdon, equation (133). If the mainstream Mach number is near unity the term

$$(1-M^2)\frac{\partial^2\phi}{\partial x^2}$$

is negligible compared to the term

$$\frac{2i\omega M}{A}\frac{\partial\phi}{\partial x}.$$

This is true provided

$$|1-M| \ll \omega c/U$$

so the approximation is valid provided the frequency is high enough. The transonic small perturbation equation is therefore

$$\frac{\partial^2\phi}{\partial y^2} - \frac{2i\omega M}{A}\frac{\partial\phi}{\partial x} + \frac{\omega^2\phi}{A^2} = 0. \qquad (86)$$

This equation is also valid for blades of small thickness, provided

$$(\partial\phi/\partial x)_{\text{steady}} \ll \omega c/U$$

which leads to

$$\omega c/U \gg \delta^{2/3}.$$

This argument shows that the transonic equation is at least as good an approximation as the original acoustic equation. In fact Landahl (1961) has argued in detail that for isolated aerofoils in the transonic range the acoustic equation leads to physically inadmissable solutions, whereas the transonic equation gives the correct small pertubation solution. These arguments will be summarized here.

The one-dimensional solution of the acoustic equation, Verdon , equation (133), for flow in the chordwise direction shows two waves, one, the 'advancing wave', traveling forward at a speed of A(M+1), and the other, the 'receding wave', traveling at a speed of A(M-1). The transonic equation (86) on the other hand just shows the advancing wave traveling at a speed of 2AM, and no receding wave. Disturbances do not propagate upstream in the transonic solution.

Looking at the solution of the acoustic equation near M=1 one sees that the receding wave has a low velocity, and therefore a short wavelength. If there is a smooth distribution of sources along the chord, the effects of the receding wave will tend to cancel, as M→1, but this cancellation will not operate at the leading and trailing edges where there are discontinuities in the source distribution. If the Mach number is just above 1, the solution of the acoustic equation will show large short-wavelength oscillations propagating back from the leading edge. If the Mach number is just below 1, the solution will show large short wavelength oscillations propagating upstream from the trailing edge. These oscillations are not present in the solution of the transonic equation.

Now consider the actual steady flow over an aerofoil with small but finite thickness just below M=1. The flow will be subsonic near the leading edge, sonic near the maximum thickness point, and supersonic up to the trailing edge where there will be attached shock waves. Unsteady receding waves generated at the leading edge will go upstream, and receding waves generated at the trailing edge cannot go upstream, so no receding wave effects appear on the aerofoil from the leading and trailing edges. This behavior is quite different from the solution of the acoustic equation, but is matched by the behavior of the transonic equation. If the freestream Mach number is slightly above one, there will be a shock wave ahead of the leading edge, but the flow over the aerofoil will be the same, and the argument is unaffected (Mach number freeze).

At a somewhat lower Mach number the trailing edge shock will move upstream onto the aerofoil, and its position will oscillate dus to the effect of the unsteady flow. This situation will not be well modeled by either the acoustic equation or the transonic equation.

Landahl (1961) also shows that due to a variation of Mach number along the chord, the amplitude of the receding wave varies strongly, growing in a flow decelerating through M=1, and decaying in an accelerating flow. This is in contrast to the solution of the acoustic equation which shows a wave of constant amplitude. The transonic equation, which shows no receding wave should be a better model.

Finally Landahl (1961) considers nonlinear unsteady effects, and concludes that these will prevent the amplitude of the receding waves from becoming large and will cause them to damp out within a few wavelengths.

In cascade geometry the acoustic equation becomes unusable between Mach numbers of approximately 0.9 and 1.1. If the Mach number is raised from 0.9, maintaining the phase angle constant, an infinite series of resonances is passed on approaching M=1, and another infinite series is found just above M=1. Also, in the supersonic range, the number of wave reflections becomes infinite as M approaches 1 from above. These features make the programs discussed in the previous two sections unusable in the transonic range.

It is concluded that the transonic theory should be used for thin blades of small camber between Mach numbers of about 0.9 and 1.1, but that its use should be confined to cases when there are no significant shock waves on the blade surfaces.

The effect of Mach number in the transonic equation (86) can be removed by a transformation similar to the Prandtl-Glauert transformation used in subsonic flow. All dimensions in the y direction are scaled by the factor M. The transformed cascade therefore has a different spacing and stagger angle, but frequency parameter and phase angle are unaffected. The transonic equation then becomes

$$\frac{\partial^2\phi}{\partial y^2} - \frac{2i\omega}{U}\frac{\partial\phi}{\partial x} + \frac{\omega^2\phi}{U^2} = 0. \qquad (87)$$

It is therefore only necessary to consider the case M=1 in the following discussion.

Switching to axial and tangential axes ξ and η, the transonic equation becomes

$$\sin^2\theta\,\frac{\partial^2\phi}{\partial\xi^2} - 2\sin\theta\cos\theta\,\frac{\partial^2\phi}{\partial\xi\partial\eta} + \cos^2\theta\,\frac{\partial^2\phi}{\partial\eta^2}$$

$$- \frac{2i\omega}{U}\left(\frac{\partial\phi}{\partial\xi}\cos\theta + \frac{\partial\phi}{\partial\eta}\sin\theta\right) + \frac{\omega^2}{U^2}\phi = 0.$$

If we now look for a solution of the form $\phi = \phi \exp i(\alpha\xi + \beta\eta)$, we find that the wave numbers are related by

$$\alpha^2\sin^2\theta - 2\alpha\beta\sin\theta\cos\theta + \beta^2\cos^2\theta$$

$$- \frac{2\omega}{U}(\alpha\cos\theta + \beta\sin\theta) - \frac{\omega^2}{U^2} = 0.$$

Since β is determined by the phase angle, this is a quadratic equation for α, and may be solved to give

$$(U\alpha/\omega) = \{\cos\theta\,[(U\beta/\omega)\sin\theta + 1]) \pm$$

$$[2(U\beta/\omega)\sin\theta + 1]^{1/2}\}/\sin^2\theta$$

and resonance occurs when $(U\beta/\omega) = -1/(2\sin\theta)$.

There is therefore only one value of phase angle for resonance. If β exceeds this value, (assuming positive stagger angle), α is real and propagating waves occur. If β is less than this value, α is complex and decaying waves occur. This resonance is associated with the advancing wave. The multiple resonances associated with the receding wave have been suppressed.

The transonic solution for zero stagger angle and 180° phase angle has been given by Savkar (1976) using Laplace transform methods. This is the case of a single aerofoil vibrating in a wind tunnel. He concludes that the degree of interference from the tunnel walls is weaker than would be thought of at first.

A transonic solution for general stagger angle and phase angle has been given by Surampudi and Adamczyk (1984, 1985) using the Wiener-Hopf procedure. It is shown that the transonic solution joins on smoothly to the subsonic and supersonic solutions at Mach numbers of 0.9 and 1.1. It is found that bending vibration is always stable, but that torsional flutter is predicted. It is found that increasing the frequency parameter and decreasing the stagger angle and solidity have a stabilizing effect on torsional flutter.

The transonic solution therefore fills in the gap between the subsonic and supersonic solutions. It is however likely that real effects such as shock waves and boundary layers will have a much larger effect than in the subsonic and supersonic regimes.

A transonic solution for zero stagger and arbitrary phase angle was developed by Schlein (1975) and Platzer et al (1976). This approach was based on the time-linearized transonic flow theory delineated by Verdon in this volume. Neglecting the product terms on the right-hand side of Verdon's equation (147) and introducing the approximations

$$\bar{\phi}_x = 0 \quad \text{and} \quad (\gamma+1)\,\bar{\phi}_{xx} = \text{Const} = \lambda > 0$$

a linear parabolic equation is obtained, following Oswatitsch and Keune (1955) and Teipel (1964).

Three different methods of solution were developed using Laplace and Fourier-transform techniques as well as a collocation technique. The inversion technique due to Hamamoto (1960) proved to be the computationally most efficient procedure. The collocation technique was based on previous work by Gorelov (1966) for supersonic oscillating cascades. Computed stability boundaries showed increased regions of instability with decreasing blade spacing.

ACTUATOR DISC THEORY

Actuator disc theory applies to certain special cases of the more general theory discussed in previous sections, and in these cases it will be found possible to derive analytic results in closed form. There are two fundamental limitations.

The first of these is that the time taken for the fluid to flow through the cascade must be small compared with the time for one oscillation of the flow. This is equivalent to assuming that the frequency parameter λ must be small,

$$\lambda = \omega c/U << 1.$$

The second fundamental limitation is that the interblade phase angle must be small,

$$|\sigma| << 1.$$

In general λ and σ will be of the same order of magnitude. The wavelength of the disturbance in the chordwise (x) direction is $2\pi c/\lambda$ and the wavelength in the tangential (η) direction is $2\pi s/\sigma$, so that these wavelengths are comparable.

These assumptions enable the flow to be considered from two viewpoints. First there is a picture (Figure 5), drawn to a scale comparable with the wavelength of the disturbance, in which the blades are very small, and the cascade is equivalent to an actuator disc. A second picture, similar to Figure 1, may be drawn to a scale comparable to the blade chord, and this just shows a few of the blades near the origin of Figure 5. In this second picture the flow may be regarded as quasi-steady, and any kind of steady flow cascade data can be used.

In the actuator disc plane, and upstream of the actuator disc, the perturbations consist of just one of the acoustic wave solutions discussed in "Fundamental Acoustic Wave Solutions," with $r = o$ in equation (19). The solution carrying acoustic energy upstream is required. Downstream of the actuator disc, the corresponding solution carrying energy downstream is required, plus a vorticity wave as discussed in the section "Vorticity Wave Solutions."

The solution for incompressible unstalled flow through a cascade of flat plates at zero incidence has been given by Whitehead (1959), and for subsonic flow by Whitehead (1986). Three conditions from the cascade plane are required. These are for continuity, deviation, and zero stagnation pressure loss.

The continuity equation is

$$\frac{\rho_2}{\rho} + \frac{v_{r\xi 2}}{V_\xi} = \frac{\rho_1}{\rho} + \frac{v_{r\xi 1}}{V_\xi} \qquad (88)$$

where the suffix r refers to conditions relative to the blades, and suffices 1 and 2 refer to conditions just upstream and downstream of the cascade, but very near the origin in the actuator disc plane.

The condition for deviation in subsonic flow is obtained by applying the Prandtl-Glauert transformation to get an equivalent cascade in incompressible flow, and then using the known analytical result for incompressible flow in cascades of flat plates given by Durand (1934). In the Prandtl-Glauert transformation all distances parallel to the chord are unchanged, but all distances normal to the chord are reduced by a factor B, where $B^2=1-M^2$. Using a * to indicate quantities in the transformed plane, the stagger and space/chord ratio are given by

$$\tan(\theta^*) = \tan(\theta)/B \ , \text{ and}$$
$$(s^*/c) = B\,(s/c)\cos(\theta)/\cos(\theta^*) \ . \qquad (89)$$

The deviation is then given by

$$v_{ry_2} = b\, v_{ry_1} \ . \qquad (90)$$

This equation holds in both the original and the transformed planes. The constant b is related to the space/chord ratio and the stagger angle in the transformed plane as follows

$$\pi c/s^* = -\cos\theta^* \ln b + 2\sin\theta^* \tan^{-1}$$
$$\{(1-b)\tan\theta^*/(1+b)\} \qquad (91)$$

For closely spaced blades, $b = 0$ is a good approximation.

The condition for zero stagnation pressure loss is

$$p_{ro2} = p_{ro1} \qquad (92)$$

where the suffix zero means a stagnation pressure.

Equations (88), (89) and (91) apply for the flow relative to the blades in the cascade plane. When these equations are combined with the actuator disc plane equations, the whole set may be solved.

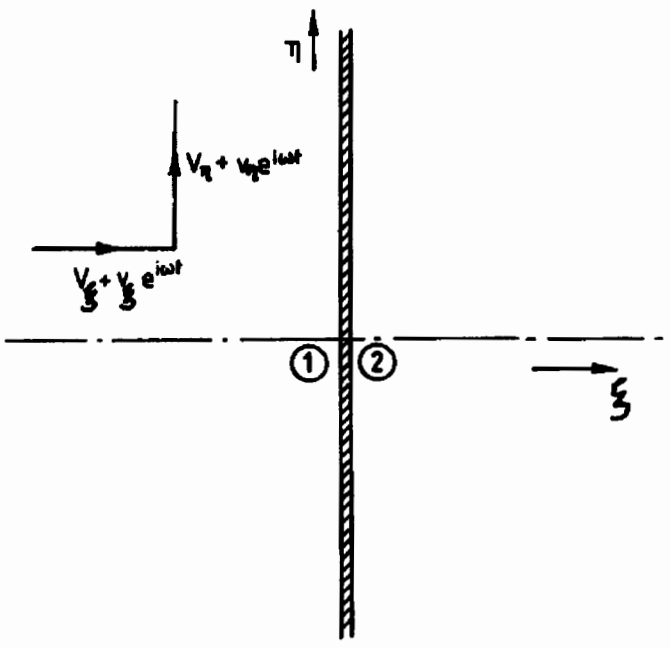

Fig. 5. Actuator Disc Plane.

Results from actuator disc theory depend on the ratio of phase angle to frequency, although both of these quantities are individually small. It is therefore convenient to write

$$\mu = \sigma U/\omega s = \sigma c/\lambda s. \qquad (93)$$

The result for the blade force due to blade vibration with velocity h_y in the y direction is then

$$f_y/\bar{\rho}Uch_y = \frac{-2T\ E\ (1-b)}{-b\ H + I + K} \qquad (94)$$

where

$$E = (\mu^2+2\mu\sin\theta + 1)(1-M^2\cos^2\theta)$$

$$H = (P-T\sin\theta)(-R+\mu\cos\theta)$$

$$I = (P+T\sin\theta)(R+\mu\cos\theta)$$

$$K = 2T\cos\theta(1-M^2\cos^2\theta)$$

$$P = \mu\cos\theta(1-M^2\cos^2\theta)-\sin\theta\cos\theta\ M^2(1+\mu\sin\theta)$$

$$R = T(\mu+\sin\theta)$$

and

$$T = \{(\mu^2+2\mu\sin\theta+1)M^2-\mu^2\}^{1/2}$$

for propagating waves,

$$T = -i\{-(\mu^2+2\mu\sin\theta+1)M^2+\mu^2\}^{1/2}$$

for decaying waves.

The corresponding result for supersonic flow, with a subsonic axial velocity, has been given by Whitehead and Davies (1983).

In supersonic flow the continuity equation (87) is unchanged and there is no Kutta condition at the trailing edge. But provided the axial velocity is subsonic, and that case (a) in Figure 3 is excluded the incidence angle of relative flow into the cascade is zero (Kantrowitz, 1946). This condition is used instead of the deviation condition (90), and gives

$$v_{y1} = \dot{h}_y \qquad (95)$$

The result of the elimination is

$$f_y/\bar{\rho}Uch_y = \frac{2sTE}{cFG} \qquad (96)$$

$$E = (\mu^2 + 2\mu\sin\theta + 1)(1 - M^2\cos^2\theta)$$
$$F = [M^2\cos\theta(\sin\theta + \mu)-\mu\cos\theta + T\sin\theta]$$
$$G = [\mu\cos\theta - (\mu + \sin\theta)T]$$

where

$$T = -\{(\mu^2 + 2\mu\sin\theta + 1)M^2 - \mu^2\}^{1/2}$$

if

$$\mu < M/(-M\sin\theta + (1-M^2\cos^2\theta)^{1/2})$$

case of propagating waves,

$$T = -i\{(\mu^2 + 2\mu\sin\theta + 1)M^2 + \mu^2\}^{1/2}$$

if

$$M/\{-M\sin\theta + (1-M^2\cos^2\theta)^{1/2}\} < \mu$$

$$< M/\{-M\sin\theta - (1-M^2\cos^2\theta)^{1/2}\}$$

case of decaying waves,

$$T = +\{(\mu^2 + 2\mu\sin\theta + 1)M^2 - \mu^2\}^{1/2}$$

if

$$M/\{-M\sin\theta - (1 - M^2\cos^2\theta)^{1/2}\} < \mu,$$

case of propagating waves.

The force is zero at the cut-off or resonance points, where $T = 0$. The force is also zero when the axial velocity is sonic, $M\cos\theta = 1$.

These results also apply to torsional motion of the blades, with h_y replaced by $U\alpha$, and to the effect of wakes being convected into the cascade. This is because at zero frequency the upwash velocities given by equations (11), (12) and (44) are all uniform.

These results can also be used to find the moment acting on the blades. Since the cascade operates in quasi-steady flow, the force acts at the centre of pressure for steady flow in the cascade. In subsonic flow this point can be found by using thin aerofoil theory for cascades (Pistolesi, 1937). In supersonic flow the centre of pressure is a distance $(c - d_2/2)$ downstream of the leading edge, as in the section "Solutions for Supersonic Cascade."

Actuator disc theory can be extended in a number of ways. For instance, results have been obtained for incompressible flow through cascades of closely spaced blades having large amounts of turning of the mean flow. (The results given in the paper by Whitehead (1959) are wrong in this respect. The correct results are given in an appendix to the paper by Whitehead (1962). Results have also been obtained for incompressible flow through cascades of closely spaced blades having a stagnation pressure loss which varies with incidence.

The most important extension of actuator disc theory is when the restriction to small frequencies is relaxed, but the restriction to small phase angles is maintained. This is now called semi-actuator-disc theory. This method was developed by Sohngen (1953) and by Tanida and Okazaki (1963) for incompressible flow and for translational motion of the blades.

The equations for the actuator disc plane are the same as in actuator disc theory. The three equations required from the cascade plane are obtained by considering the control surface shown in Figure 6. The control surface is the space between two blades, 13'344'21, and moves at a constant speed equal to that at which the blade 12 travels at that instant. The sides of the control surface 33' and 44' are the displacement of blade 34 relative to the blade 12, and are given by

$$s' = h_y e^{i(\omega t + \sigma)} - h_y e^{i\omega t} = i\sigma h_y e^{i\omega t}$$

since σ is small.

Applying continuity to this control surface gives the result

$$v_{\xi_1} - v_{\xi_2} + (V_{n_1} - V_{n_2})(\sigma/s)\dot{h}_y \sin\theta - i(c/s)\,\sigma\dot{h}_y = 0 \,. \qquad (97)$$

Here $v_{\xi 1}$ and $v_{\xi 2}$ are the absolute unsteady axial velocities. The third term arises from the change of steady tangential velocity giving a net flow through the sides of length s', and is an actuator disc term. The last term arises from the change in gap between the blades and is a semi-actuator-disc term.

The second equation from the cascade plane is for the relative flow exit angle, and equation (90) for the relative velocity normal to the blades is unchanged. The usual approximation is $b = 0$.

The third equation relates the pressure at outlet from the cascade to the pressure at inlet. This relationship is derived in two stages. It is presumed that a loss of relative stagnation pressure occurs at the inlet to the cascade, so that

$$P_{ro1} - P_{ro3} = \tfrac{1}{2}\rho\, V_{r\xi 1}{}^2\, Z \qquad (98)$$

where the suffix 3 refers to a plane just behind the leading edges of the blades, and Z is a stagnation pressure loss coefficient which is a function of the inlet angle of flow relative to the cascade or $v_{rn1}/v_{r\xi 1}$.

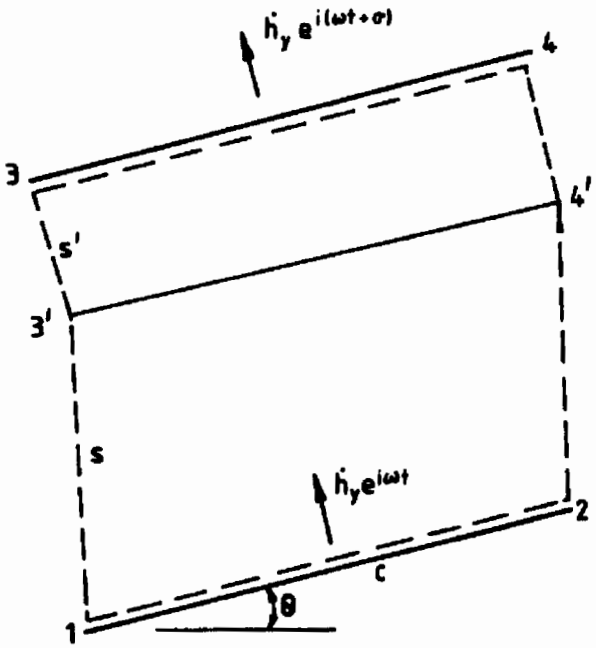

Fig. 6. Control Surface for Semi-Actuator-Disc Theory.

The relationship between the relative stagnation pressure at cascade outlet (plane 2) and at plane 3 is obtained by integrating the equation of motion in the x direction along the passage between two adjacent blades to give

$$P_{ro3} - P_{ro2} = i\omega\bar{c}\, v_{rx} \,. \qquad (99)$$

With the addition of a momentum equation in the η direction, which relates the blade force to the flow variables, a complete set of linear equations is available and may be solved. The result is too lengthy to give here, but may be found in the paper by Tanida and Okazaki (1963).

Semi-actuator-disc theory has been extended to compressible subsonic flow. The case of transmission and reflection of sound waves by a cascade, and the generation of sound waves due to an incoming vorticity wave, have been treated by Kaji and Okazaki (1970). The effects of compressibility on flutter in subsonic flow have been considered by Kaji and Okazaki (1972).

Semi-actuator-disc theory has been extended to supersonic flow by Kaji (1980), and in a somewhat different way by Adamczyk (1978).

The semi-actuator-disc theories are probably the most useful available for stalled flow. But they do require experimental or empirical input giving the nature of the loss function Z. Actual stalling processes take a finite time to develop. The theories can be extended to allow for a time lag, but again experimental or empirical information must be provided to determine the time constant.

SINGULARITY THEORY

We now turn to a quite different way of building up solutions for the unsteady flow through cascades by the superposition of simple analytical solutions. In this case, the solutions are restricted to lossless incompressible flow, but they apply to blades with large amounts of thickness and camber. The particular method which will be sketched in the following is largely taken from a paper by Atassi and Akai (1980).

The potential flow past any number of two-dimensional bodies of arbitrary shape may be represented as being due to a distribution of singularities placed around the boundaries of the bodies. The singularities may be either a distribution of sources and sinks (plus at least one vortex for each body if that body has circulation) or a distribution of vortices (plus at least one source or sink if the body has a net flow out or in from the surface). A further alternative is to use doublets. A distribution of doublets placed around the boundary and directed along the boundary is equivalent to a distribution of sources and sinks, and a distribution of doublets directed normal to the boundary is equivalent to a distribution of vortices (provided there is no net flow out or in from the surface and no net circulation). The well-known Martensen (1959) method for steady flow

in cascades uses a distribution of vortices round the surfaces of the blades. In this case the notional flow inside the contours of the surfaces has zero velocity, so that the strength of the vortices can be arranged to make the tangential velocity just inside the contour equal to zero. For the unsteady case however, the velocity normal to the surface just outside the surface is used as a boundary condition. Also, since in the unsteady case there is vorticity shed from the blades into the wake, it is necessary to use an additional distribution of vortices along the wakes of the blades.

In order to handle singularity theory it is convenient to work in a complex z plane where $z = x + iy$. It is then necessary to change the notation slightly and make all the unsteady variables proportional to $\exp(j\omega t)$. The unsteady variables are then hypercomplex numbers, which have four components, a real component, an i component, a j component, and an ij component. ($i^2 = -1$, $j^2 = -1$, but we must not write $ij = -1$).

If there is a source density distribution m on the surface at the point z , so that the source strength for a length of surface $\delta\tau$ is $m\delta\tau$, then the velocities induced at a point z^1 not on the surface are given by

$$v_x - iv_y = \frac{1}{2\pi} \int \frac{m d\tau}{z^1 - z} \qquad (100)$$

where the integral is taken over the surfaces of all blades and their wakes.

Similarly for a vorticity distribution γ_t , the induced velocities at z^1 are given by

$$v_x - iv_y = \frac{1}{2\pi i} \int \frac{\gamma_t d\tau}{z^1 - z} \quad . \qquad (101)$$

In general any combination of source and vorticity distribution may be used. Equations (100) and (101) may therefore be combined to give

$$v_x - iv_y = \frac{1}{2\pi i} \int \frac{(\gamma_t + im)d\tau}{z^1 - z} = \frac{1}{2\pi i} \oint \frac{\mu_m dz}{z^1 - z} \qquad (102)$$

where the integral is now a contour integral taken anticlockwise round the blade surface. μ_m is a complex singularity strength. If $\mu_m dz$ is real it corresponds to pure vorticity, and if $\mu_m dz$ is imaginary it corresponds to a pure source-sink distribution.

Equation (102) gives the induced velocities at a point z^1 which is not on the surface. If z^1 is on the surface the integral is singular and the induced velocities just outside the surface are given by

$$v_x - iv_y = \frac{1}{2\pi i} \oint \frac{\mu_m(z)dz}{z - z^1} - \frac{1}{2} \mu_m(z^1) \qquad (103)$$

and the induced velocities just inside the surface are given by

$$v_x - iv_y = \frac{1}{2\pi i} \oint \frac{\mu_m(z)dz}{z - z^1} + \frac{1}{2} \mu_m(z^1) \quad . \qquad (104)$$

The extra terms on the right hand side of these equations give a jump in tangential velocity across the surface equal to the strength of the vortex sheet at the surface and a jump in normal velocity across the surface equal to the strength of the source-sink distribution along the surface.

Since the cascade is assumed to be vibrating with an inter-blade phase angle σ , the singularity strength on the mth blade at $z + mse^{i\theta}$ is given by

$$\mu_m = \mu_o e^{jm\sigma}$$

Hence the velocities induced just outside a point z^1 on the reference blade are

$$v_x - iv_y = \frac{1}{2\pi i} \sum_{m=-\infty}^{+\infty} \oint \frac{\mu_o(z)e^{jm\sigma}dz}{z + mse^{i\theta} - z^1} - \frac{1}{2} \mu_o(z^1) \qquad (105)$$

where the contour integral is now taken round the reference blade $m = 0$.

The series can be summed analytically to give the induced velocities just outside z^1 as

$$v_x - iv_y = \frac{1}{2\pi i} \oint K(z - z^1)\mu_o(z)dz - \frac{1}{2} \mu_o(z^1) \qquad (106)$$

where

$$K(z^*) = \frac{\pi e^{j(\pi-\sigma)z^*}}{se^{i\theta}\sin(\pi z^*)} \quad 0 < \sigma < 2\pi \; . \qquad (107)$$

This is a more general form of equation (14). The integral in equation (106) is taken round the reference blade and its wake.

The contour integral of μ_o round the reference blade is

$$\oint \mu_o dz = \oint (\gamma_t + im)d\tau = \Gamma_o \qquad (108)$$

where Γ_o is the circulation round the reference blade, and the integral of the source term is zero since there is no net flow out of the blade surface.

Verdon's equation (75) gives the jump in potential across the wake as

$$\left[\!\left[\phi\right]\!\right] = \left[\!\left[\phi\right]\!\right]_{TE} e^{-j\omega(\Delta - \Delta_{TE})} \qquad (109)$$

where Δ is the drift function, defined so that the difference in Δ between any two points on the same mean streamline is equal to the time for a particle to move from one point to the other under the influence of the mean flow. In this case

$$\Delta - \Delta_{TE} = \int_{\tau_{TE}}^{\tau} V_\tau^{-1} \, d\tau \qquad (110)$$

which gives the time taken for fluid to flow from the trailing edge to the point in question on the wake, and the integral is taken along the wake line.

The jump in potential across the wake at the trailing edge is just the circulation, so that

$$\left[\!\left[\phi\right]\!\right]_{TE} = \Gamma_o \ . \qquad (111)$$

Differentiating equation (109) with respect to distance along the wake then gives

$$\left[\!\left[\frac{\partial \phi}{\partial \tau}\right]\!\right] = \left[\!\left[v_\tau\right]\!\right] = \gamma_t = -j\omega \Gamma_o \frac{\partial A}{\partial \tau}$$
$$e^{-j\omega(A-A_{TE})} = -j\omega\Gamma_o V_\tau^{-1} e^{-j\omega(A-A_{TE})} \ . \qquad (112)$$

This equation gives the strength of the vortex sheet at any point in the wake.

The boundary condition to be satisfied just outside the blade surface is given by Verdon's equation (69). For rigid body motion of the blades, the displacement vector is given by Verdon's equation (102) and the normal velocity just outside the blade surface reduces to

$$v_n = j\omega \overset{\bullet}{r}.\overset{\bullet}{n} + \alpha V_\tau - (\overset{\bullet}{r}.\nabla \overset{\bullet}{V}).\overset{\bullet}{n}, \qquad (113)$$

where

$$\overset{\bullet}{r} = h + \overset{\bullet}{\alpha} \times \overset{\bullet}{R_p} \ . \qquad (114)$$

The integral equation for μ_o is therefore

$$\left[\frac{1}{2\pi i} \oint K(z-z^1)\mu_o(z)dz - \frac{j\omega\Gamma_o}{2\pi i} \int K(z-z^1)\right.$$
$$\left. V_\tau^{-1} e^{-j\omega(A-A_{TE})} d\tau - \frac{1}{2} \mu_o(z^1)\right] .\overset{\bullet}{n}$$
$$= j\omega \overset{\bullet}{r}.\overset{\bullet}{n} + \alpha V_\tau - (\overset{\bullet}{r}.\nabla \overset{\bullet}{V}).\overset{\bullet}{n} \qquad (115)$$

where the first integral is taken anticlockwise around the reference blade, and the second integral is taken along the wake of the reference blade from the trailing edge to downstream infinity. Γ_o is related to μ_o by equation (108). This equation has to be solved, subject to the additional Kutta condition at the trailing edge, which specifies that μ_o must not be infinite at that point.

Details of a solution method are given in the paper by Atassi and Akai (1980). The first move is to solve for the steady flow. Then for the unsteady flow equation (115) is solved numerically. The last term on the right hand side of equation (115), which arises from the translation of a point on the blade surface through the mean velocity field, may be singular at the trailing edge and exhibits large values round the leading edge. This is a source of numerical difficulty. Atassi and Akai (1980) overcame the difficulty essentially by writing

$$\mu_o^1(z) = \mu_o(z) + \overset{\bullet}{r}.\nabla \overset{\bullet}{V} \ . \qquad (116)$$

By using μ_o^1 as the primary measure of the unknown singularity strength instead of μ_o, the awkward last term on the righthand side of equation (115) may be cancelled.

The complex singularity strength μ_o may in principle be any combination of source and vorticity strengths. This arbitrariness corresponds to the idea that whereas the flow outside the blade surfaces is fixed by the physics of the problem, the notional flow inside the blade surfaces may be chosen in any convenient way. Atassi and Akai (1980) therefore choose to make μ_o^1 real with respect to the space variables. The singularity therefore corresponds to pure vorticity when the surface is parallel to the x (chordwise) axis, and to pure source or sinks when the surface is parallel to the y axis.

The integral equation (115) is solved numerically by matching the normal velocities at N points round the blade surface, where N must correspond to the number of points at which the singularity strength is specified. Once the singularity strength has been found, the velocity and pressure distributions just outside the blade surface may be found. The pressure distributions are then integrated to give the aerodynamic forces and moment.

Due to a programming error, the results for the real part of the pressure distributions given in the paper by Atassi and Akai (1980) are not correct. Results for which the error has been corrected are given by Akai and Atassi (1981).

SPECIMEN RESULTS FOR FLAT PLATE CASCADES

In order to specify the unsteady performance of cascades of flat plates, five independent non-dimensional variables are necessary. These are the space to chord ratio, the stagger angle, the Mach number, the frequency parameter, and the interblade phase angle. Excluding the acoustic information, and the detail of the pressure distributions, there are twelve dependent variables of interest. These are the real and imaginary components of the force and moment for bending, torsion, and wakes. This number of variables makes any general presentation of the results totally impractical, and it is only possible to present specimen results. It is therefore necessary to have computer programs available so that any particular cases of interest can be calculated.

For incompressible flow, tables of specimen results have been made by Whitehead (1960). Figure 7 illustrates the force coefficient due to bending for a space to chord ratio of unity and a stagger angle of 60°. In this and the following figures the axes are the real and imaginary parts of the force coefficient, and lines of constant frequency parameter and phase angle are shown. In general the lines of constant frequency parameter form closed loops as the phase angle is varied. However, the line of zero frequency parameter is not closed for finite phase angles. In order to close the loop actuator disc theory, with various values of σ/λ in the limit $\sigma \to 0$ and $\lambda \to 0$, must be used, and the result for this is shown on Figure 7.

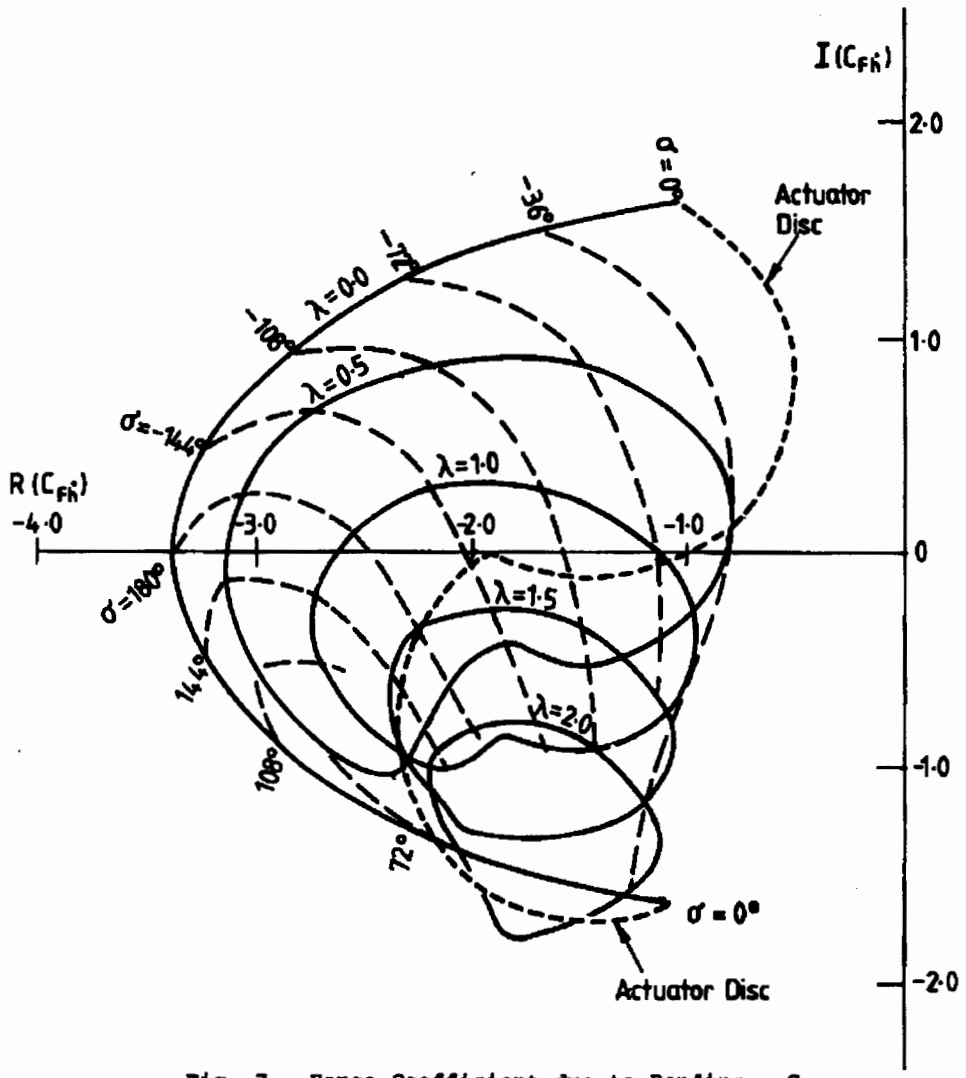

Fig. 7. Force Coefficient due to Bending. C_{Fh} s/c=1.0, θ=60°, M=0.0.

Similar results for the same cascade in subsonic compressible flow are shown in Figure 8 (for a Mach number of 0.5) and on Figure 9 (for a Mach number of 0.8). The presentation of results for compressible flow is made difficult by the very wild behaviour of the coefficients which occurs near the acoustic resonances. For this reason the real and imaginary parts of the force coefficient are plotted separately against phase angle on figures 9a and 9b. One resonance on these figures at $\lambda = 0.5$ and $\sigma = 102.45°$ is shown in detail. The other resonances are merely indicated as discontinuities in the curves. Only the parts of the loops of constant frequency parameter which are in the well-behaved sub-resonant region are shown on the figures. Figure 8 also shows the actuator disc case: there is also a range of values of σ/λ for which C_{Fh} is purely real, so that the line lies along the real axis. Figure 9 at the higher Mach number of 0.8 illustrates the wild fluctuations which occur near the resonance point at the frequency parameter of 0.5, but at the higher frequency parameters the results steady down and become much less dependent on frequency parameter and phase angle.

Specimen results for two supersonic cascades are shown in Figures 10 and 11. These cascades are examples used by Verdon and McCuns (1975) which have been rather widely used as test cases. Cascade A (Figure 10) has the wave pattern illustrated in figure 3b, whereas Cascade B (Figure 11) has the additional internal wave reflections illustrated in Figure 3c. On these figures the wild behaviour near the acoustic resonance has been largely suppressed, but on Figure 10 the complete loop for a frequency parameter of 0.602 is shown and illustrates typical behaviour.

Pure bending flutter of a system with no mechanical damping is predicted if the real part of the force coefficient due to bending is positive. Figures 7 to 11 show that the real part of this coefficient is alway negative, so that pure bending vibration is damped. This behaviour has always been found for flat plate cascades at zero incidence. However, actuator-disc and semi-actuator-disc analyses allowing for steady deflection of the steady flow through the cascade do show the possibility of pure bending flutter.

Pure torsional flutter depends on a further parameter, which is the position along the chord of the torsional axis. Torsional flutter is predicted by these theories if the frequency parameter is sufficiently low. The effect of compressibility of the fluids is generally found to be stabilizing as the Mach number increases in the subsonic range. But there is also a theoretical possibility of "resonance flutter", over a very narrow range of interblade phase angle close to the acoustic resonance condition at comparatively high frequency parameters (Whitehead 1973). Whether this is a real danger on practical machines is not known.

CONCLUSIONS

This chapter has presented what are regarded as the most important two-dimensional solutions which can be obtained by the superposition of elementary analytical solutions. This has enabled cascades of flat plates to be treated up to Mach numbers at which the axial velocity becomes sonic. Also, singularity theory, valid for incompressible flow through cascades of thick cambered blades, has been discussed in the section "Singularity Theory" and actuator disc theory, valid at low frequencies and for small phase angles, in the section "Actuator Disc Theory." These methods enable useful predictions to be made for the vibration characteristics of real blades. But for turbine blade sections with a lot of turning and with high Mach numbers or for compressor blades having strong shock waves in the flow, these methods are hardly adequate, and it is necessary to go to field methods. These will be discussed in the Chapter, "Numerical Methods for Unsteady Transonic Flow."

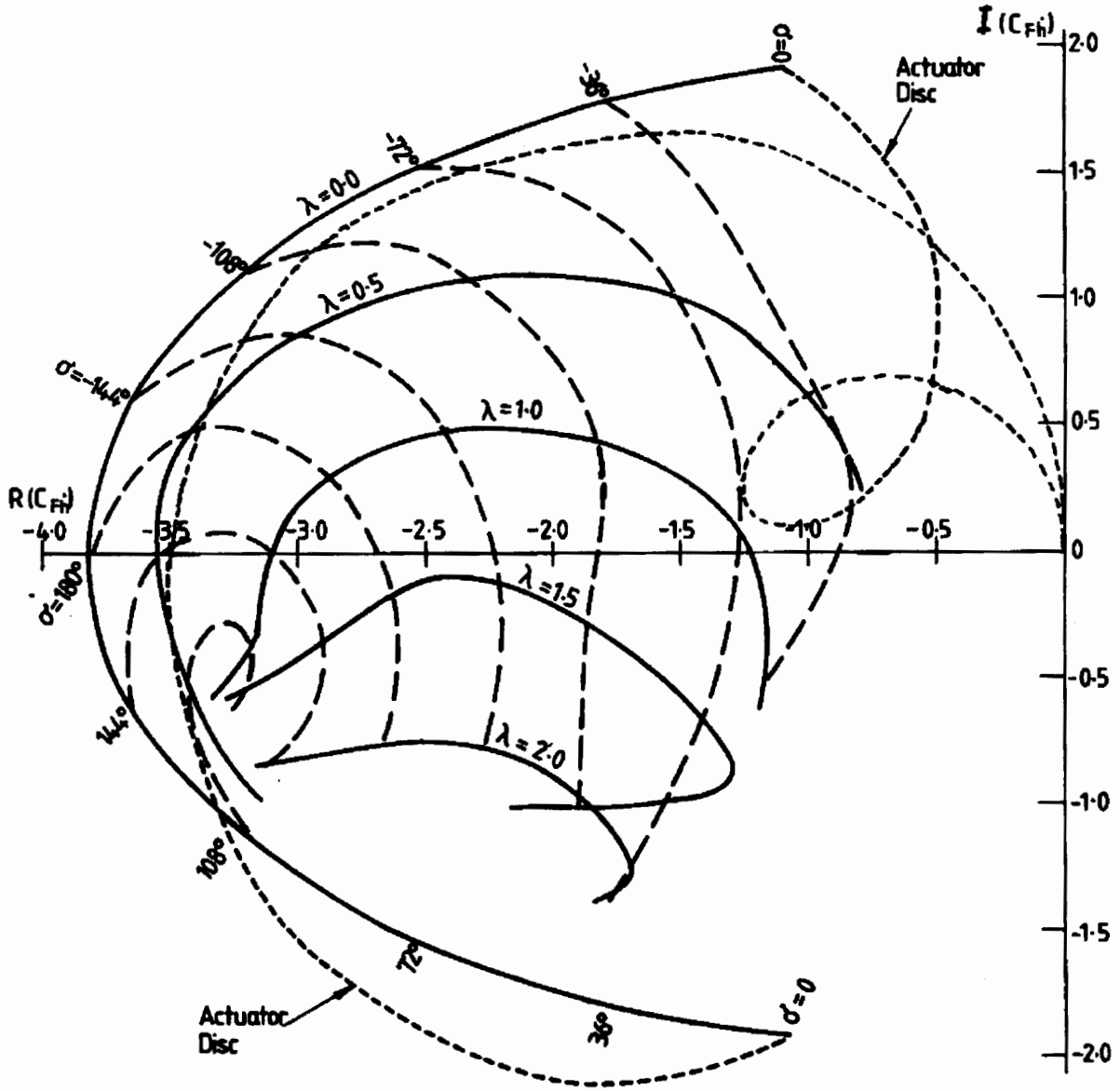

Fig. 8. Force Coefficient due to Bending. C_{Fh} s/c=1.0, θ=60°, M=0.5.

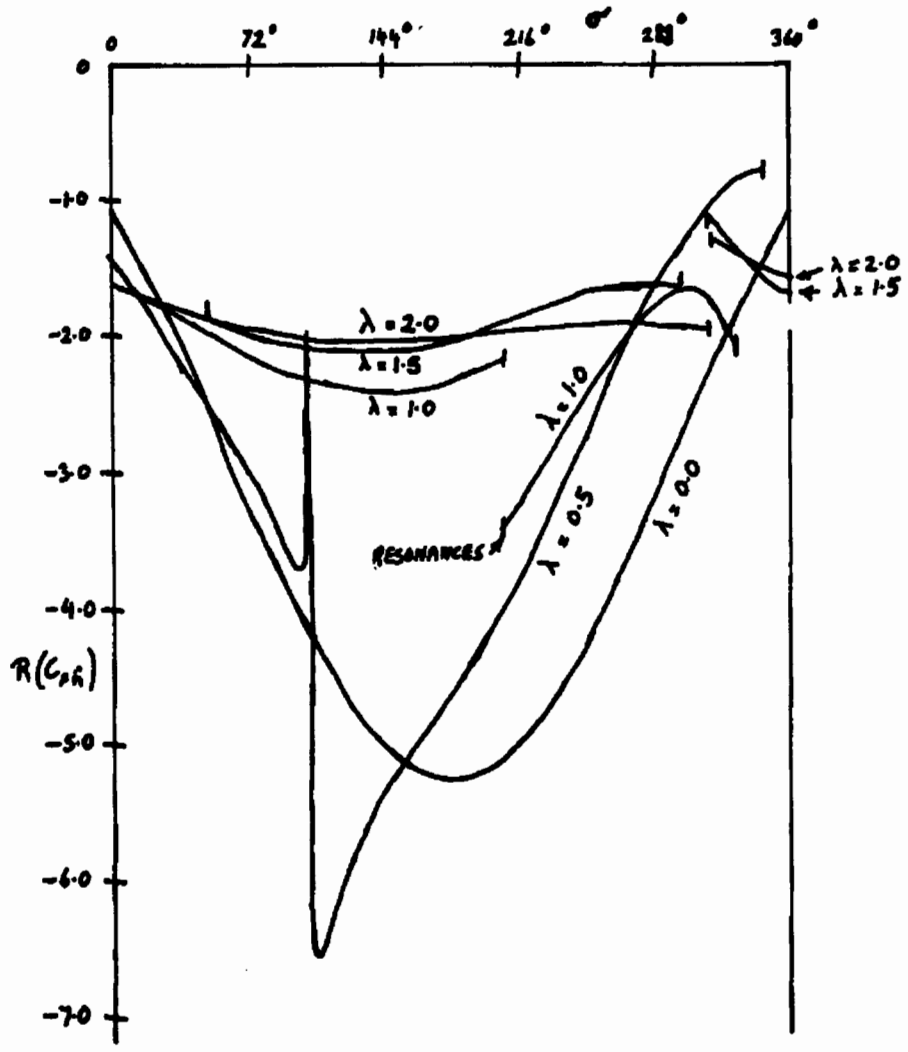

Fig. 9a. Force Coefficient due to Bending. $C_{F\dot{h}}$ Real Part.
s/c=1.0, θ=60°, M=0.8.

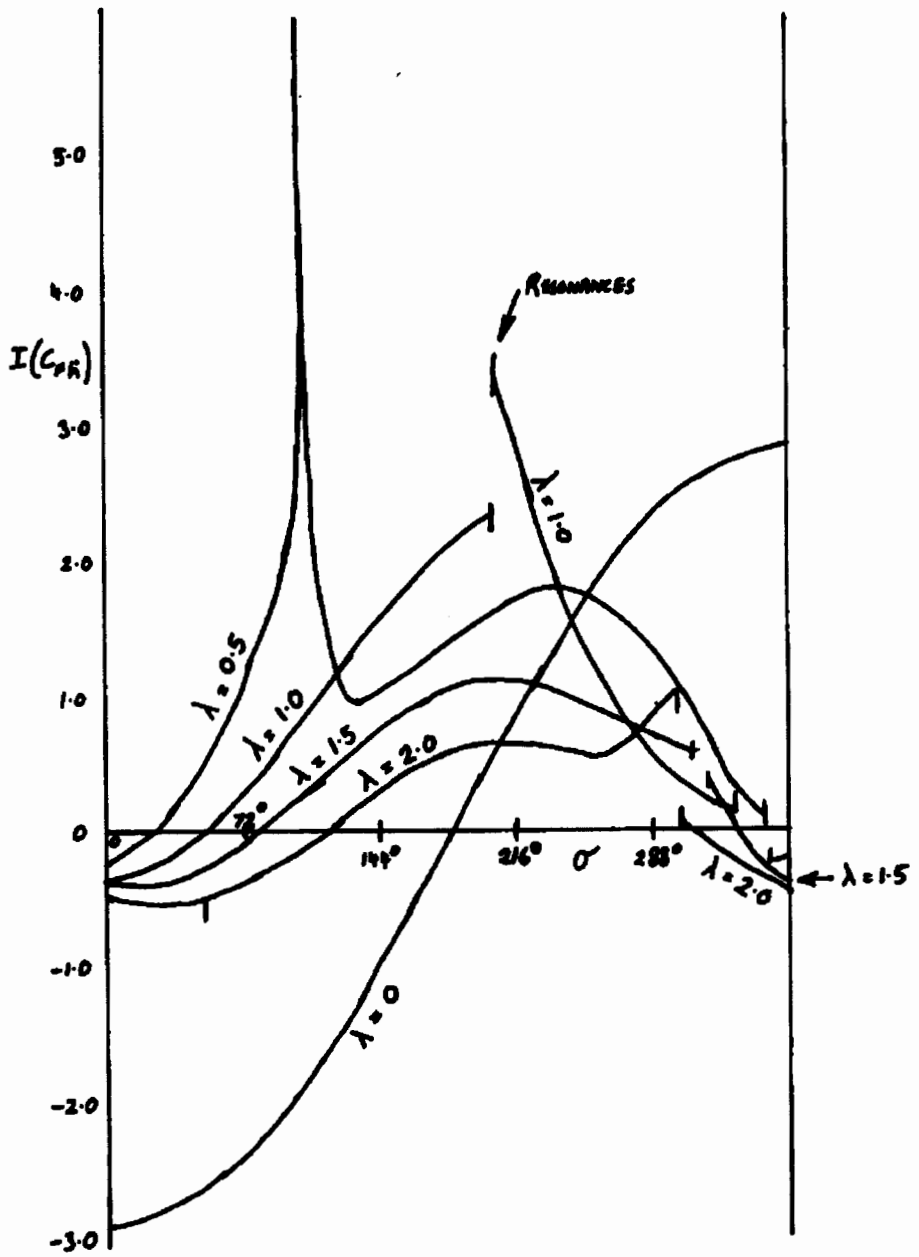

Fig. 9b. Force Coefficient due to Bending. $C_{F\dot{h}}$ Imaginary Part. s/c=1.0, θ=60°, M=0.8.

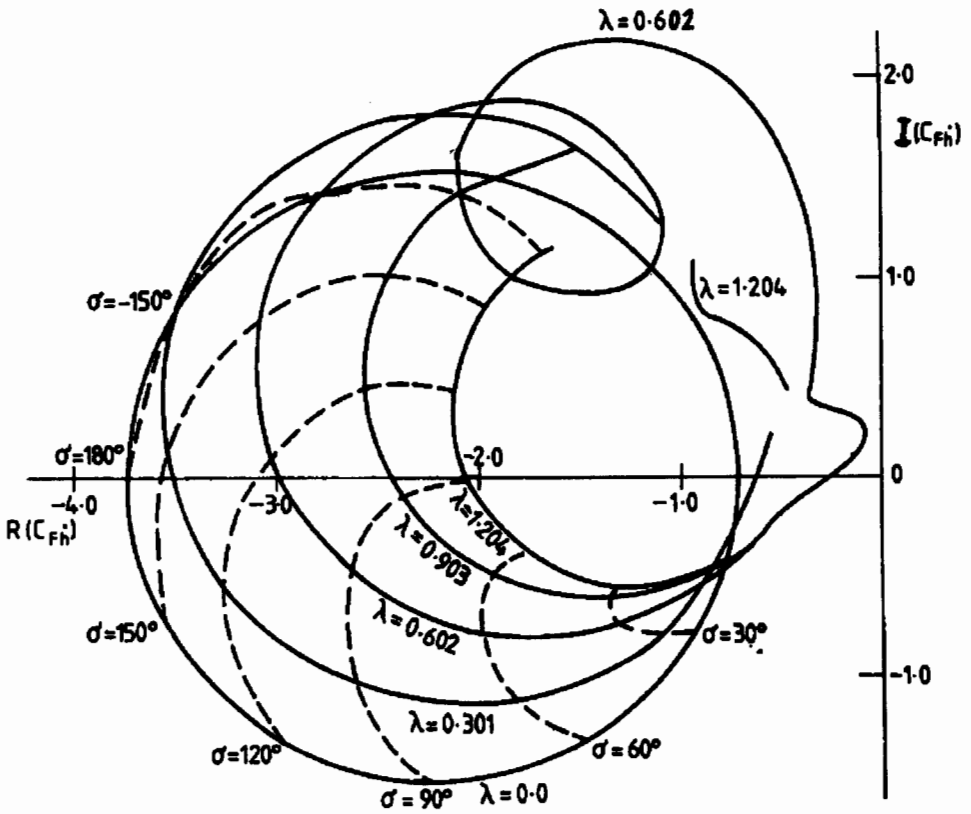

Fig. 10. Force Coefficient due to Bending. C_{Fh}
s/c=0.7889, =59.53°, M=1.3454.

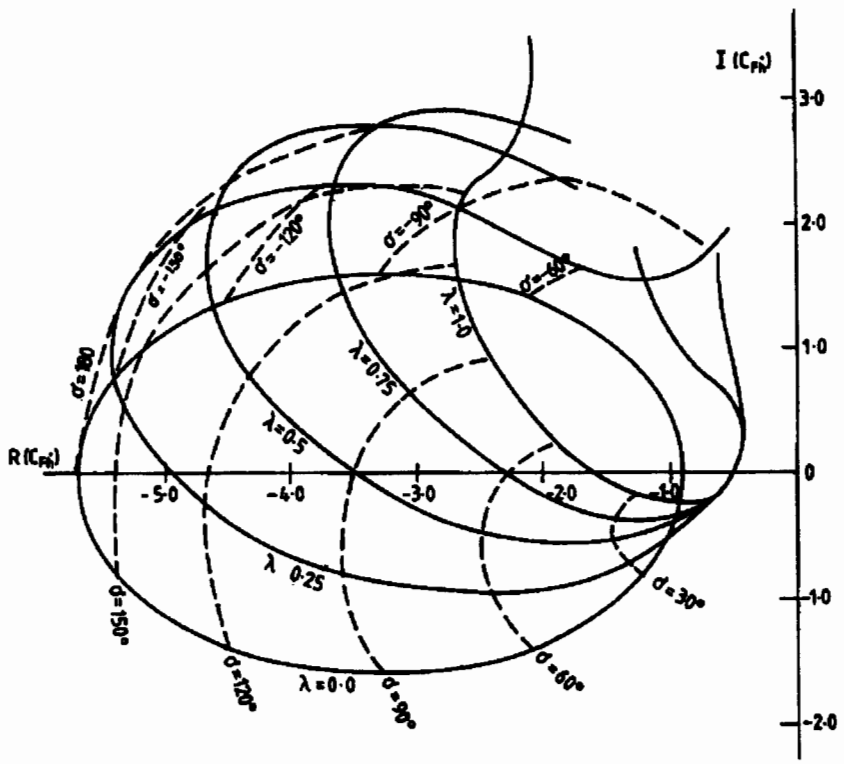

Fig. 11. Force Coefficient due to Bending. C_{Fh}
s/c=0.6708, =63.43°, M=1.2806.